

Collective fields in the functional renormalization group for fermions, Ward identities, and the exact solution of the Tomonaga-Luttinger model

Florian Schütz,¹ Lorenz Bartosch,^{1,2} and Peter Kopietz¹

¹*Institut für Theoretische Physik, Universität Frankfurt,
Robert-Mayer-Strasse 8, 60054 Frankfurt, Germany*

²*Department of Physics, Yale University, P.O.Box 208120, New Haven, CT 06520-8120, USA*

(Dated: September 17, 2004)

We develop a new formulation of the functional renormalization group (RG) for interacting fermions. Our approach unifies the purely fermionic formulation based on the Grassmannian functional integral, which has been used in recent years by many authors, with the traditional Wilsonian RG approach to quantum systems pioneered by Hertz [Phys. Rev. B 14, 1165 (1974)], which attempts to describe the infrared behavior of the system in terms of an effective bosonic theory associated with the soft modes of the underlying fermionic problem. In our approach, we decouple the interaction by means of a suitable Hubbard-Stratonovich transformation (following the Hertz-approach), but do not eliminate the fermions; instead, we derive an exact hierarchy of RG flow equations for the irreducible vertices of the resulting coupled field theory involving both fermionic and bosonic fields. The freedom of choosing a momentum transfer cutoff associated with the bosonic soft modes in addition to the usual band cutoff associated with the fermions opens the possibility of new RG schemes. In particular, we show how the exact solution of the Tomonaga-Luttinger model (i.e., one-dimensional fermions with linear energy dispersion and interactions involving only small momentum transfers) emerges from the functional RG if one works with a momentum transfer cutoff. Then the Ward identities associated with the local particle conservation at each Fermi point are valid at every stage of the RG flow and provide a solution of an infinite hierarchy of flow equations for the irreducible vertices. The RG flow equation for the irreducible single-particle self-energy can then be closed and can be reduced to a linear integro-differential equation, the solution of which yields the result familiar from bosonization. We suggest new truncation schemes of the exact hierarchy of flow equations, which might be useful even outside the weak coupling regime.

PACS numbers: 71.10.-w, 71.10.Pm., 71.20.Hf

I. INTRODUCTION

In condensed matter and statistical physics the renormalization group (RG) in the form developed by Wilson and co-authors^{1,2,3} has been very successful. At the heart of this intuitively appealing formulation of the RG lies the concept of an effective action describing the physical properties of a system at a coarse grained scale. Conceptually, the derivation of this effective action is rather simple provided the theory can be formulated in terms of a functional integral: one simply integrates out the degrees of freedom describing short-wavelength fluctuations in a certain regime, and subsequently rescales the remaining degrees of freedom in order to compare the new effective action with the original one. Of course, in practice, the necessary functional integration can almost never be performed analytically, so that one has to resort to some approximate procedure.⁴ However, if the elimination of the short wavelength modes is performed in infinitesimal steps, one can write down in closed form a formally exact RG flow equation describing the change of the effective action due to mode elimination and rescaling. The earliest version of such a functional RG equation has been derived by Wegner and Houghton.⁵ Subsequently, many authors have derived alternative versions of the functional RG with the same physical content, using different types of generating functionals. In particular, the advan-

tages of working with the generating functional of the one-particle irreducible vertices have been realized early on by Di Castro, Jona-Lasinio, and Peliti,⁶ and by Nicoll, Chang, and Stanley.^{7,8} Note that the focus of the above works was an accurate description of second order phase transitions at finite temperatures, where quantum mechanics is irrelevant.

In recent years, there has been much interest in quantum systems exhibiting phase transitions as a function of some non-thermal control parameter, such as pressure or density. In a pioneering paper, Hertz⁹ showed how the powerful machinery of the Wilsonian RG can be generalized to study quantum critical phenomena in Fermi systems. Technically, this is achieved with the help of so-called Hubbard-Stratonovich transformations, which replace the fermionic two-particle interaction by a suitable bosonic field that couples to a quadratic form in the fermion operators.¹⁰ The fermions can then be integrated out in a formally exact way, resulting in an effective action for the bosonic field. Of course, there are many possible ways of decoupling fermionic two-body interactions by means of Hubbard-Stratonovich transformations. In the spirit of the usual Ginzburg-Landau approach to classical critical phenomena, one tries to construct the effective bosonic theory such that the field can be identified with the fluctuating order parameter, or its field conjugate. However, if the system supports soft modes other than the order parameter and if these modes couple to the

order parameter,^{11,12} an attempt to construct an effective field theory in terms of the order parameter alone leads in general to an effective action with singular and non-local vertices, so that the usual RG methods developed for classical phase transitions cannot be applied. In this case, it is better to construct an effective action involving all soft modes explicitly. However, for a given problem the nature of the soft modes is not known a priori, so that the explicit introduction of the corresponding degrees of freedom by means of a suitable Hubbard-Stratonovich transformation is always based on some prejudice about the nature of the ground state and the low-lying excitations of the system.

In order to avoid this problem and to have a completely unbiased RG approach for interacting fermions, one can also apply the Wilsonian RG directly to the Grassmannian functional integral representation of the partition function or the Green functions of an interacting Fermi system.¹³ In the past ten years, several groups have further developed this method.^{14,15,16,17,18,19,20,21,22,23,24,25,26} In particular, the mode elimination step of the RG transformation has been elegantly cast into formally exact differential equations for suitably defined generating functionals. These functional equations then translate to an infinite hierarchy of integro-differential equations for the vertices. On the technical level, it is often advantageous to work with the generating functional of the one-particle irreducible vertices.^{6,7,8} For classical field theories the exact RG flow equation for this generating functional has been obtained by Wetterich,²⁷ and by Morris.²⁸ For non-relativistic fermions, the corresponding flow equation has been derived by Salmhofer and Honerkamp¹⁸ and, independently and in more explicit form, by Kopietz and Busche.¹⁹

However, the purely fermionic formulation of the Wilsonian RG has several disadvantages. In order to obtain at least an approximate solution of the formally exact hierarchy of RG flow equations for the vertices, severe truncations have to be made, which can only be justified as long as the fermionic four-point vertex (i.e., the effective interaction) remains small. Hence, in practice the fermionic functional RG is restricted to the weak coupling regime, so that possible strong coupling fixed points are not accessible within this method. Usually, one-loop truncated RG equations are iterated until at least one of the marginal interaction constants becomes large, which is then interpreted as a weak-coupling instability of the Fermi system in the corresponding channel.^{15,16,17}

Within the framework of the Wilsonian functional RG a consistent two-loop calculation has not been performed so far due to the immense technical difficulties involved. Such a calculation should also take into account the frequency dependence of the effective interaction and the self-energy corrections to the internal Green functions. Note that in the work by Katanin and Kampf²⁵ the frequency dependence of the effective interaction has been ignored, so that the effect of possible

bosonic collective modes is not included in these calculations. It is well known that two-loop calculations are more conveniently performed using the field-theoretical RG method, provided the physical problem of interest can be mapped onto a renormalizable field theory. Ferraz and co-authors^{29,30} recently used the field-theoretical RG to calculate the single-particle Green function at the two loop level for a special two-dimensional Fermi system with a flat Fermi surface. Interestingly, they found a new non-Fermi liquid fixed point characterized by a finite renormalized effective interaction and a vanishing wave-function renormalization. Note that the bare interaction diverges in this model, but the divergence is canceled by the vanishing wave-function renormalization such that the renormalized interaction remains finite.

Another difficulty inherent in any RG approach to Fermi systems at finite densities arises from the fact that the true Fermi surface of the interacting many-body system is not known a priori. In fact, in dimensions $D > 1$ interactions can even change the symmetry of the Fermi surface.^{31,32} In a perturbative approach, finding the renormalized Fermi surface is a delicate self-consistency problem³³; if one starts from the wrong Fermi surface one usually encounters unphysical singularities.³⁴ So far, the self-consistent renormalization of the Fermi surface has not been included in the numerical analysis of the one-loop truncated fermionic functional RG. As shown in Refs. 19, 21, and 30, the renormalized Fermi surface can be defined as a fixed point of the RG and can in principle be calculated self-consistently entirely within the RG framework.

The progress in overcoming the above difficulties inherent in the RG approach to fermions using a purely fermionic parameterization has been rather slow. In our opinion, this has a simple physical reason: the low lying excitations (i.e., soft modes) of an interacting Fermi system consist not only of fermionic quasi-particles, but also of bosonic collective excitations.³⁵ The latter are rather difficult to describe within the purely fermionic parameterizations used in Refs. 14,15,16,17,18,19,20,21,22,23,24,25,26. Naturally, a formulation of the functional RG where both fermionic and bosonic excitations are treated on equal footing should lead to a more convenient parameterization. Such a strategy seems also natural in the light of the observation by Kirkpatrick, Belitz, and co-workers¹¹ (see also Ref. 12) that an effective low-energy and long-wavelength action with well-behaved vertices is only obtained if the soft modes are not integrated out, but appear explicitly as quantum fields.

The aim of this work is to set up a functional renormalization group scheme that allows for a simultaneous treatment of fermionic as well as collective bosonic degrees of freedom. This is done by explicitly decoupling the interaction via a Hubbard-Stratonovich transformation in the spirit of Hertz⁹ and then considering the functional renormalization group equations for the mixed field theory involving both fermionic and bosonic fields. This type of approach has been suggested previously by Correia,

Polonyi, and Richert,³⁶ who studied the homogeneous electron gas by means of a gradient expansion of a functional version of a Callan-Symanzik equation. Here, we follow the more standard approach and derive a hierarchy of flow equations for the vertex functions of our coupled Fermi-Bose theory. A related approach has also been developed by Wetterich and co-authors.^{37,38} However, they discussed only a simple truncation of the exact hierarchy of RG flow equations involving an effective potential in a bosonic sector and a momentum-independent Yukawa-coupling. They did not pay any attention to the problem of the compatibility of the RG flow with Ward identities, which play a crucial role for interacting fermions with dominant forward scattering. Our procedure bridges the gap between the purely bosonic approach to quantum critical phenomena by Hertz⁹ and the purely fermionic functional RG method developed in the past decade by several authors.^{14,15,16,17,18,19,20,21,22,23,24,25,26} Contrary to the approach by Hertz,⁹ in our approach the fermionic degrees of freedom are still present, so that the feedback of the collective bosonic modes on the one-particle spectral properties of the fermions can be studied.

The parameterization of the low-lying excitations of an interacting Fermi system in terms of collective bosonic fields is most natural in one spatial dimension,^{39,40} where Fermi liquid theory breaks down and is replaced by the Luttinger liquid concept.⁴⁰ An exactly solvable paradigm of a Luttinger liquid is the Tomonaga-Luttinger model (TLM),⁴¹ consisting of fermions with exactly linear energy dispersion and interactions involving only small momentum transfers. A description in terms of bosonic variables is well known to provide an exact solution for thermodynamic quantities as well as correlation functions.³⁹ One might then wonder if it is also possible to obtain the complete form of the correlation functions of the TLM entirely within the framework of the functional RG. An attempt²⁰ to calculate the momentum- and frequency dependent single-particle spectral function $A(k, \omega)$ of the TLM by means of an approximate iterative two-loop solution of the functional RG equations at weak coupling yields the correct behavior of $A(\pm k_F, \omega)$ known from bosonization (where k_F is the Fermi momentum), but yields incorrect threshold singularities for momenta away from $\pm k_F$. In this work we go considerably beyond Ref. 20 and show how the TLM can be solved *exactly* using our mixed fermionic-bosonic functional RG. A crucial point of our method is that the RG can be set up in such a way that the Ward identities underlying the exact solubility of the TLM^{42,43,44,45} are preserved by the RG. Note that this is not the case in the purely fermionic formulation of the functional RG.²⁶

Very recently, Benfatto and Mastropietro⁴⁷ also developed an implementation of the RG for the TLM which takes the asymptotic Ward identities into account. However, these authors did not introduce bosonic collective fields and did not attempt to calculate the exact single particle Green function.

The rest of the paper is organized as follows. In Sec. II,

we introduce the model, carry out the decoupling of the interaction and set up a compact notation which turns out to facilitate the bookkeeping in the derivation of the functional RG equations which is presented in detail in Sec. III. In the central Sec. IV, we introduce a new RG scheme which uses the momentum transfer of the effective interaction as a cutoff. We show that for linearized energy dispersion the resulting infinite hierarchy of flow equations for the irreducible vertices involving two external fermion legs and an arbitrary number of external boson legs can be solved exactly by means of an infinite set of Ward identities. Using these identities, the flow equation for the irreducible self-energy can then be reduced to a closed linear integro-differential equation, which can be solved exactly. In one dimension, we recover in Sec. IV C the exact solution of the Tomonaga-Luttinger model in the form familiar from functional bosonization^{45,46}. Finally, in Sec. V, we summarize our results and give a brief outlook on possible further applications of our method. There are three appendices where we present some more technical details. In Appendix A, we use our compact notation introduced in Sec. II to discuss the structure of the tree expansion in our coupled Fermi-Bose theory. Appendix B contains a derivation of the skeleton diagrams for the first few irreducible vertices of our theory using the Dyson-Schwinger equations of motion, which follow from the invariance of the functional integral with respect to infinitesimal shift-transformations. Finally, in Appendix C we use the gauge invariance of the mixed Fermi-Bose action to derive the infinite set of Ward identities involving vertices with two fermion legs and an arbitrary number of boson legs.

II. INTERACTING FERMIONS AS COUPLED FERMI-BOSE SYSTEMS

In this section we discuss the Hubbard-Stratonovich transformation and set up a condensed notation to treat fermionic and bosonic fields on the same footing. This will allow us to keep track of the rather complicated diagrammatic structure of the flow equations associated with our coupled Fermi-Bose system in a very efficient way. A similar notation has been used previously in Refs. 18 and 38.

A. Hubbard-Stratonovich transformation

We consider a normal fermionic many-body system with two-particle density-density interactions. In the usual Grassmannian functional integral approach¹⁰ the grand-canonical partition function and all (imaginary)-time-ordered Green functions can be represented as func-

tional averages involving the following Euclidean action,

$$S[\bar{\psi}, \psi] = S_0[\bar{\psi}, \psi] + S_{\text{int}}[\bar{\psi}, \psi], \quad (2.1)$$

$$S_0[\bar{\psi}, \psi] = \sum_{\sigma} \int_K \bar{\psi}_{K\sigma} [-i\omega + \xi_{\mathbf{k}\sigma}] \psi_{K\sigma}, \quad (2.2)$$

$$S_{\text{int}}[\bar{\psi}, \psi] = \frac{1}{2} \sum_{\sigma\sigma'} \int_{\bar{K}} f_{\mathbf{k}}^{\sigma\sigma'} \bar{\rho}_{\bar{K}\sigma} \rho_{\bar{K}\sigma'}, \quad (2.3)$$

where the composite index $K = (i\omega, \mathbf{k})$ contains a fermionic Matsubara frequency $i\omega$ as well as an ordinary wave vector \mathbf{k} . Here the energy dispersion $\xi_{\mathbf{k}\sigma} = \epsilon_{\mathbf{k}\sigma} - \mu$ is measured relative to the chemical potential, and $f_{\mathbf{k}}^{\sigma\sigma'}$ are some momentum-dependent interaction parameters. Throughout this paper, labels with a bar refer to bosonic frequencies and momenta, while labels without a bar refer to fermionic ones. We have normalized the Grassmann fields $\psi_{K\sigma}$ and $\bar{\psi}_{K\sigma}$ such that the integration measure in Eq. (2.1) is

$$\int_K = \frac{1}{\beta V} \sum_{\omega, \mathbf{k}} \xrightarrow{\beta, V \rightarrow \infty} \int \frac{d\omega}{2\pi} \frac{d^D k}{(2\pi)^D}, \quad (2.4)$$

where β is the inverse temperature and V is the volume of the system. The Fourier components of the density are represented by the following composite field

$$\rho_{\bar{K}\sigma} = \int_K \bar{\psi}_{K\sigma} \psi_{K+\bar{K},\sigma}, \quad (2.5)$$

which implies $\bar{\rho}_{\bar{K}\sigma} = \rho_{-\bar{K}\sigma}$. The discrete index σ is formally written as a spin projection, but will later on also serve to distinguish right and left moving fields in the Tomonaga-Luttinger model. This is why a dependence of the dispersion $\xi_{\mathbf{k}\sigma}$ on σ has been kept.

The interaction is bilinear in the densities and can be decoupled by means of a Hubbard-Stratonovich transformation.⁴⁵ The interaction is then mediated by a real field φ and the resulting action reads

$$S[\bar{\psi}, \psi, \varphi] = S_0[\bar{\psi}, \psi] + S_0[\varphi] + S_1[\bar{\psi}, \psi, \varphi], \quad (2.6)$$

where the free bosonic part is given by

$$S_0[\varphi] = \frac{1}{2} \sum_{\sigma\sigma'} \int_{\bar{K}} [f_{\mathbf{k}}^{-1}]^{\sigma\sigma'} \varphi_{\bar{K}\sigma}^* \varphi_{\bar{K}\sigma'}, \quad (2.7)$$

and the coupling between Fermi and Bose fields is

$$\begin{aligned} S_1[\bar{\psi}, \psi, \varphi] &= i \sum_{\sigma} \int_{\bar{K}} \bar{\rho}_{\bar{K}\sigma} \varphi_{\bar{K}\sigma} \\ &= i \sum_{\sigma} \int_K \int_{\bar{K}} \bar{\psi}_{K+\bar{K},\sigma} \psi_{K\sigma} \varphi_{\bar{K}\sigma}. \end{aligned} \quad (2.8)$$

Note that the Fourier components of a real field satisfy $\varphi_{\bar{K}\sigma}^* = \varphi_{-\bar{K}\sigma}$. For the manipulations in the next section it will prove advantageous to further condense the notation and collect the fields in a vector $\Phi = (\psi, \bar{\psi}, \varphi)$. The

quadratic part of the action can then be written in the symmetric form

$$\begin{aligned} S_0[\Phi] &= S_0[\bar{\psi}, \psi] + S_0[\varphi] = -\frac{1}{2} \left(\Phi, [\mathbf{G}_0]^{-1} \Phi \right) \\ &= -\frac{1}{2} \int_{\alpha} \int_{\alpha'} \Phi_{\alpha} [\mathbf{G}_0]_{\alpha\alpha'}^{-1} \Phi_{\alpha'}, \end{aligned} \quad (2.9)$$

where \mathbf{G}_0 is now a matrix in frequency, momentum, spin and field-type indices, and α is a “super label” for all of these indices. The symbol \int_{α} denotes integration over the continuous components and summation over the discrete components of α . The matrix \mathbf{G}_0^{-1} has the block structure

$$\mathbf{G}_0^{-1} = \begin{pmatrix} 0 & \zeta [\hat{G}_0^{-1}]^T & 0 \\ \hat{G}_0^{-1} & 0 & 0 \\ 0 & 0 & -\hat{F}_0^{-1} \end{pmatrix}, \quad (2.10)$$

where⁴⁸ $\zeta = -1$ and \hat{G}_0 and \hat{F}_0 are infinite matrices in frequency, momentum and spin space, with matrix elements

$$[\hat{G}_0]_{K\sigma, K'\sigma'} = \delta_{K, K'} \delta_{\sigma\sigma'} G_{0,\sigma}(K), \quad (2.11)$$

$$[\hat{F}_0]_{\bar{K}\sigma, \bar{K}'\sigma'} = \delta_{\bar{K}+\bar{K}', 0} F_{0,\sigma\sigma'}(\bar{K}'), \quad (2.12)$$

where

$$G_{0,\sigma}(K) = [i\omega - \xi_{\mathbf{k}\sigma}]^{-1}, \quad (2.13)$$

$$F_{0,\sigma\sigma'}(\bar{K}) = f_{\mathbf{k}}^{\sigma\sigma'}. \quad (2.14)$$

The Kronecker $\delta_{K, K'} = \beta V \delta_{\omega, \omega'} \delta_{\mathbf{k}, \mathbf{k}'}$ appearing in Eqs. (2.11,2.12) is normalized such that it reduces to Dirac δ -functions $\delta_{K, K'} \rightarrow (2\pi)^{D+1} \delta(\omega - \omega') \delta^{(D)}(\mathbf{k} - \mathbf{k}')$ in the limit $\beta, V \rightarrow \infty$. Note that the bare interaction plays the role of a free bosonic Green function. For later reference, we note that the inverse of Eq. (2.10) is

$$\mathbf{G}_0 = \begin{pmatrix} 0 & \hat{G}_0 & 0 \\ \zeta \hat{G}_0^T & 0 & 0 \\ 0 & 0 & -\hat{F}_0 \end{pmatrix}, \quad (2.15)$$

and that the transpose of \mathbf{G}_0 satisfies

$$\mathbf{G}_0^T = \mathbf{Z} \mathbf{G}_0 = \mathbf{G}_0 \mathbf{Z}, \quad (2.16)$$

where the “statistics matrix” \mathbf{Z} is defined by

$$[\mathbf{Z}]_{\alpha\alpha'} = \delta_{\alpha\alpha'} \zeta_{\alpha}. \quad (2.17)$$

Here, $\zeta_{\alpha} = -1$ if the super-index α refers to a Fermi field, and $\zeta_{\alpha} = 1$ if α labels a Bose field.

B. Generating functionals

1. Generating functional of connected Green functions

We now introduce sources J_{α} and define the generating functional $\mathcal{G}[J]$ of the Green functions as follows,

$$\mathcal{G}[J] = e^{\mathcal{G}_c[J]} = \frac{1}{Z_0} \int D\Phi e^{-S_0 - S_1 + (J, \Phi)}. \quad (2.18)$$

Here, $\mathcal{G}_c[J]$ is the generating functional for connected Green functions and the partition function \mathcal{Z}_0 of the non-interacting system can be written as the Gaussian integral

$$\mathcal{Z}_0 = \int D\Phi e^{-S_0}. \quad (2.19)$$

We use again the compact notation

$$(J, \Phi) = \int_{\alpha} J_{\alpha} \Phi_{\alpha}. \quad (2.20)$$

Usually, the source terms for fields of different types are written out explicitly in the form¹⁰

$$\begin{aligned} (J, \Phi) &= (\bar{j}, \psi) + (\bar{\psi}, j) + (J^*, \varphi) = \\ &\sum_{\sigma} \int_K \bar{j}_{K\sigma} \psi_{K\sigma} + \sum_{\sigma} \int_K \bar{\psi}_{K\sigma} j_{K\sigma} + \sum_{\sigma} \int_{\bar{K}} J_{\bar{K}\sigma}^* \varphi_{\bar{K}\sigma}. \end{aligned} \quad (2.21)$$

A comparison between Eq. (2.20) and Eq. (2.21) shows that the sources in the compact notation are related to the standard ones by $J = (\bar{j}, \zeta j, J^*)$. The connected n -line Green functions $\mathcal{G}_{c,\alpha_1 \dots \alpha_n}^{(n)}$ are then defined via the functional Taylor expansion

$$\mathcal{G}_c[J] = \sum_{n=0}^{\infty} \frac{1}{n!} \int_{\alpha_1} \dots \int_{\alpha_n} \mathcal{G}_{c,\alpha_1 \dots \alpha_n}^{(n)} J_{\alpha_1} \cdot \dots \cdot J_{\alpha_n}, \quad (2.22)$$

implying

$$\mathcal{G}_{c,\alpha_1 \dots \alpha_n}^{(n)} = \left. \frac{\delta^{(n)} \mathcal{G}_c[J]}{\delta J_{\alpha_1} \dots \delta J_{\alpha_n}} \right|_{J=0}. \quad (2.23)$$

In particular, the exact Green function of our interacting system is given by

$$[\mathbf{G}]_{\alpha\alpha'} = -\left. \frac{\delta^{(2)} \mathcal{G}_c}{\delta J_{\alpha} \delta J_{\alpha'}} \right|_{J=0} = -\mathcal{G}_{c,\alpha'\alpha}^{(2)}, \quad (2.24)$$

which we shall write in compact matrix notation as

$$\mathbf{G} = -\left. \frac{\delta^{(2)} \mathcal{G}_c}{\delta J \delta J} \right|_{J=0} = \begin{pmatrix} 0 & \hat{G} & 0 \\ \zeta \hat{G}^T & 0 & 0 \\ 0 & 0 & -\hat{F} \end{pmatrix}. \quad (2.25)$$

For the last equality, it has been assumed that no symmetry breaking occurs. Note that \mathbf{G} has the same block structure as the non-interacting \mathbf{G}_0 so that, similarly to Eq. (2.16),

$$\mathbf{G}^T = \mathbf{Z} \mathbf{G} = \mathbf{G} \mathbf{Z}. \quad (2.26)$$

In the non-interacting limit ($S_1 \rightarrow 0$) one easily verifies by elementary Gaussian integration that the matrix \mathbf{G} given in Eq. (2.24) reduces to \mathbf{G}_0 as defined in Eq. (2.15). The self-energy matrix also has the same block structure

as the inverse free propagator. Dyson's equation then reads

$$\mathbf{G}^{-1} = \mathbf{G}_0^{-1} - \boldsymbol{\Sigma}, \quad (2.27)$$

where the matrix $\boldsymbol{\Sigma}$ contains the one-fermion-line irreducible self-energy $\Sigma_{\sigma}(K)$ and the one-interaction-line irreducible polarization $\Pi_{\sigma}(\bar{K})$ in the following blocks,

$$\boldsymbol{\Sigma} = \begin{pmatrix} 0 & \zeta[\hat{\Sigma}]^T & 0 \\ \hat{\Sigma} & 0 & 0 \\ 0 & 0 & \hat{\Pi} \end{pmatrix}, \quad (2.28)$$

where

$$[\hat{\Sigma}]_{K\sigma, K'\sigma'} = \delta_{K, K'} \delta_{\sigma\sigma'} \Sigma_{\sigma}(K), \quad (2.29)$$

$$[\hat{\Pi}]_{\bar{K}\sigma, \bar{K}'\sigma'} = \delta_{\bar{K} + \bar{K}', 0} \delta_{\sigma\sigma'} \Pi_{\sigma}(\bar{K}'). \quad (2.30)$$

These matrices are spin-diagonal because the bare coupling $S_1[\psi, \bar{\psi}, \varphi]$ between Fermi and Bose fields in Eq. (2.8) is diagonal in the spin index. The blocks of the full Green function matrix \mathbf{G} in Eq. (2.25) contain the exact single-particle Green function and the effective (screened) interaction,

$$[\hat{G}]_{K\sigma, K'\sigma'} = \delta_{K, K'} \delta_{\sigma\sigma'} G_{\sigma}(K), \quad (2.31)$$

$$[\hat{F}]_{\bar{K}\sigma, \bar{K}'\sigma'} = \delta_{\bar{K} + \bar{K}', 0} F_{\sigma\sigma'}(\bar{K}'), \quad (2.32)$$

with

$$G_{\sigma}(K) = [G_{0,\sigma}^{-1}(K) - \Sigma_{\sigma}(K)]^{-1}, \quad (2.33)$$

$$F_{\sigma\sigma'}(\bar{K}) = [\hat{F}_0^{-1} + \hat{\Pi}]_{-\bar{K}\sigma, \bar{K}\sigma'}^{-1}. \quad (2.34)$$

2. Generating functional of one-line irreducible vertices

Below, we shall derive exact functional RG equations for the one-line irreducible vertices of our coupled Fermi-Bose theory. Note that the diagrammatic perturbation theory consists of both fermion and boson lines, and we require irreducibility with respect to both types of lines. We call this one-line irreducibility. Keeping in mind that a boson line represents the two-body electron-electron interaction which is screened by zero-sound bubbles for small momentum transfers, this means that for small momentum transfers our vertices are not only one-particle irreducible with respect to the one-electron lines, but also two-particle irreducible in the zero-sound channel. In order to obtain the generating functional of the corresponding irreducible vertices, we perform a Legendre transformation with respect to all field components, introducing the classical field⁴⁹

$$\Phi_{\alpha} = \frac{\delta \mathcal{G}_c}{\delta J_{\alpha}}. \quad (2.35)$$

After inverting this relation for $J = J[\Phi]$ we may calculate the Legendre effective action

$$\mathcal{L}[\Phi] = (J[\Phi], \Phi) - \mathcal{G}_c[J[\Phi]]. \quad (2.36)$$

From this we obtain

$$J_\alpha = \zeta_\alpha \frac{\delta \mathcal{L}}{\delta \Phi_\alpha}, \quad (2.37)$$

which we may write in compact matrix notation as

$$J = \mathbf{Z} \frac{\delta \mathcal{L}}{\delta \Phi}. \quad (2.38)$$

In this notation the chain rule simply reads

$$\frac{\delta}{\delta \Phi} = \frac{\delta^{(2)} \mathcal{L}}{\delta \Phi \delta \Phi} \mathbf{Z} \frac{\delta}{\delta J}. \quad (2.39)$$

Applying this to both sides of Eq. (2.35) we obtain

$$\mathbf{1} = \frac{\delta \Phi}{\delta \Phi} = \frac{\delta^{(2)} \mathcal{L}}{\delta \Phi \delta \Phi} \mathbf{Z} \frac{\delta^{(2)} \mathcal{G}_c}{\delta J \delta J}. \quad (2.40)$$

For vanishing fields Φ and J this yields

$$\frac{\delta^{(2)} \mathcal{L}}{\delta \Phi \delta \Phi} \Big|_{\Phi=0} = -\mathbf{Z} \mathbf{G}^{-1} = -[\mathbf{G}^{-1}]^T. \quad (2.41)$$

The advantage of our compact notation is now obvious: the minus signs associated with the Grassmann fields can be neatly collected in the “statistics matrix” \mathbf{Z} . If the Grassmann sources are introduced in the conventional way,¹⁰ the minus signs generated by commuting two Grassmann fields are distributed in a more complicated manner in the matrices of second derivatives.^{19,36}

From Eq. (2.41) it is evident that we need to subtract the free action from $\mathcal{L}[\Phi]$ to obtain the generating functional for the irreducible vertex functions,

$$\Gamma[\Phi] = \mathcal{L}[\Phi] - S_0[\Phi] = \mathcal{L}[\Phi] + \frac{1}{2}(\Phi, [\mathbf{G}_0^{-1}]\Phi). \quad (2.42)$$

Then we have, using the Dyson equation (2.27),

$$\begin{aligned} \frac{\delta^{(2)} \Gamma}{\delta \Phi \delta \Phi} \Big|_{\Phi=0} &= \frac{\delta^{(2)} \mathcal{L}}{\delta \Phi \delta \Phi} \Big|_{\Phi=0} + [\mathbf{G}_0^{-1}]^T \\ &= -[\mathbf{G}^{-1}]^T + [\mathbf{G}_0^{-1}]^T = \mathbf{\Sigma}^T. \end{aligned} \quad (2.43)$$

In general, the one-line irreducible vertices are defined as coefficients in an expansion of $\Gamma[\Phi]$ with respect to the fields,

$$\Gamma[\Phi] = \sum_{n=0}^{\infty} \frac{1}{n!} \int_{\alpha_1} \dots \int_{\alpha_n} \Gamma_{\alpha_1, \dots, \alpha_n}^{(n)} \Phi_{\alpha_1} \dots \Phi_{\alpha_n}. \quad (2.44)$$

The vertices $\Gamma^{(n)}$ have the same symmetry with respect to interchange of the indices as the monomial in the fields, i.e., the interchange of two neighboring Fermi fields yields a minus sign. Graphically, we represent the vertices $\Gamma^{(n)}$ by an oriented circle with n external legs, as shown in Fig. 1. With the definition (2.44) and Eq. (2.43) we have $\Gamma_{\alpha\alpha'}^{(2)} = [\mathbf{\Sigma}]_{\alpha'\alpha}$. The fact that also the higher-order vertices $\Gamma^{(n)}$ defined in Eq. (2.44) are indeed one-line irreducible (i.e., cannot be separated into two parts by cutting a single fermion line or a single interaction line) can be shown iteratively by generating a tree expansion from higher order derivatives of Eq. (2.40). We show this explicitly in Appendix A.

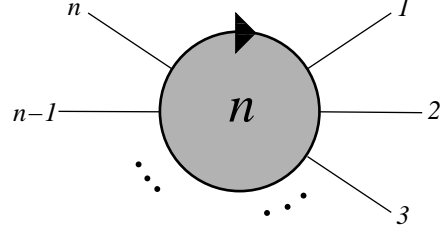


FIG. 1: Graphical representation of the symmetrized one-line irreducible n -point vertex defined via Eq. (2.44). Because for fermions the order of the indices is important (exchanging two neighboring fermion legs will generate a minus sign) the circles representing the irreducible vertices have an arrow that points to the leg corresponding to the first index; subsequent indices are arranged in the order indicated by the arrow. External legs denote either outgoing fermions ($\bar{\psi}$), incoming fermions (ψ), or bosons (φ).

III. FUNCTIONAL RG FLOW EQUATIONS FOR ONE-LINE IRREDUCIBLE VERTICES

In this section we derive exact RG flow equations for the generating functional of the one-line irreducible vertices of our coupled Fermi-Bose theory. We also classify the various vertices of the theory based on their scaling dimensions and propose a new truncation scheme involving the building blocks of the skeleton diagrams for fermionic and bosonic two-point functions.

A. Cutoff schemes

Since the interaction now appears as a propagator of the field φ , it is possible to introduce a momentum-transfer cutoff in the interaction on the same footing as a band cutoff. Note that a bandwidth cutoff restricts the relevant fermionic degrees of freedom to the vicinity of the Fermi surface, and appears to be most natural in the RG approach to fermions in one spatial dimension.⁵⁰ In higher dimensions, the Wilsonian idea of eliminating the degrees of freedom in the vicinity of the Fermi surface is implemented by defining for each momentum \mathbf{k} an associated \mathbf{k}_F by means of a suitable projection onto the Fermi surface¹⁹ and then integrating over fields with momenta in the energy shell $v_0 \Lambda < |\epsilon_{\mathbf{k}} - \epsilon_{\mathbf{k}_F}| < v_0 \Lambda_0$, where $\epsilon_{\mathbf{k}}$ is the energy dispersion in the absence of interactions. Here v_0 is some suitably defined velocity (for example some average Fermi velocity), which we introduce to give Λ units of momentum. We shall refer to $v_0 \Lambda$ as bandwidth cutoff. Formally, we introduce such a cutoff into our theory by substituting for the free fermionic Green function in Eq. (2.13)

$$\begin{aligned} G_{0,\sigma}(K) &\longrightarrow \Theta(\Lambda < D_K < \Lambda_0) G_{0,\sigma}(K) \\ &= \frac{\Theta(\Lambda < D_K < \Lambda_0)}{i\omega - \xi_{\mathbf{k}\sigma}}, \end{aligned} \quad (3.1)$$

with

$$D_K = |\epsilon_{\mathbf{k}} - \epsilon_{\mathbf{k}_F}|/v_0. \quad (3.2)$$

Here $\Theta(\Lambda < x < \Lambda_0) = 1$ if the logical expression in the brackets is true, and $\Theta(\Lambda < x < \Lambda_0) = 0$ if the logical expression is false. Ambiguities associated with the sharp Θ -function cutoff can be avoided by smoothing out the Θ -functions and taking the sharp cutoff limit at the end of the calculation.²⁸ In order to construct a consistent scaling theory, the \mathbf{k}_F in Eq. (3.2) should refer to the true Fermi surface of the interacting system, which can in principle be obtained self-consistently from the condition that the RG flows into a fixed point.^{19,21}

The above bandwidth-cutoff procedure has several disadvantages. On the one hand, for any finite value of the cutoff parameter Λ the Ward identities are violated.²⁶ Moreover, the RG flow of two-particle response functions probing the response at small momentum transfers (such as the compressibility or the uniform magnetic susceptibility) is artificially suppressed by the bandwidth cutoff. To cure the latter problem, various other parameters have been proposed to serve as a cutoff for the RG, such as the temperature¹⁷ or even the strength of the interaction.⁵² While for practical calculations these new cutoff schemes may have their advantages, the intuitively appealing RG picture that the coarse grained parameters of the renormalized theory contain the effect of the degrees of freedom at shorter length scales and higher energies gets somewhat blurred (if not completely lost) by these new schemes.

The above mentioned problems can be elegantly avoided in our mixed Fermi-Bose theory if we work with a momentum cutoff in the bosonic sector of our theory, which amounts to replacing in Eq. (2.14)

$$\begin{aligned} F_{0,\sigma\sigma'}(\bar{K}) &\longrightarrow \Theta(\Lambda < \bar{D}_{\bar{K}} < \Lambda_0) F_{0,\sigma\sigma'}(\bar{K}) \\ &= \Theta(\Lambda < \bar{D}_{\bar{K}} < \Lambda_0) f_{\bar{\mathbf{k}}\sigma}^{\sigma\sigma'}, \end{aligned} \quad (3.3)$$

where

$$\bar{D}_{\bar{K}} = |\bar{\mathbf{k}}|. \quad (3.4)$$

Keeping in mind that the bosonic field mediates the effective interaction, it is clear that Λ is a cutoff for the momentum transfer of the interaction. This is precisely the same cutoff scheme employed in the seminal work by Hertz,⁹ who discussed also more general frequency-dependent cutoffs for the labels of the bosonic Hubbard-Stratonovich fields, corresponding to more complicated functions $\bar{D}_{\bar{K}}$ than the one given in Eq. (3.4). Moreover, in the exact solution of the one-dimensional Tomonaga-Luttinger model (abbreviated here as TLM, as already defined above) by means of a careful application of the bosonization method⁵¹ the maximal momentum transferred by the interaction appears as the natural cutoff scale.

In our RG approach we have the freedom of choosing both the bandwidth cutoff $v_0\Lambda$ and the momentum transfer cutoff Λ independently. In particular, we may even

choose to get rid of the bandwidth cutoff completely and work with a momentum-transfer cutoff only. In this work, we shall show that if the interaction involves only small momentum transfers, then the pure momentum transfer cutoff scheme indeed regularizes all infrared singularities in one dimension. Moreover and most importantly, introducing a cutoff only in the momentum transfer leads to exact RG flow equations which do not violate the Ward identities responsible for the exact solubility of the TLM. Given this fact, it is not surprising that we can solve the infinite hierarchy of RG flow equations exactly and obtain the exact single-particle Green function of the TLM within the framework of the functional RG.

B. Flow equations for completely symmetrized vertices

With the substitutions (3.1) and (3.3) the non-interacting Green function \mathbf{G}_0 and hence all generating functionals depend on the cutoff parameter Λ . We can now follow the evolution of the generating functionals as we change the cutoff. Differentiation of Eq. (2.18) with respect to Λ yields for the generating functional of the Green functions,

$$\partial_\Lambda \mathcal{G} = \left\{ \frac{1}{2} \left(\frac{\delta}{\delta J}, \partial_\Lambda [\mathbf{G}_0^{-1}] \frac{\delta}{\delta J} \right) - \partial_\Lambda \ln \mathcal{Z}_0 \right\} \mathcal{G}. \quad (3.5)$$

For the connected version $\mathcal{G}_c[J] = \ln \mathcal{G}[J]$ we obtain

$$\begin{aligned} \partial_\Lambda \mathcal{G}_c &= \frac{1}{2} \left(\frac{\delta \mathcal{G}_c}{\delta J}, \partial_\Lambda [\mathbf{G}_0^{-1}] \frac{\delta \mathcal{G}_c}{\delta J} \right) \\ &\quad + \frac{1}{2} \text{Tr} \left(\partial_\Lambda [\mathbf{G}_0^{-1}] \left[\frac{\delta^{(2)} \mathcal{G}_c}{\delta J \delta J} \right]^T \right) - \partial_\Lambda \ln \mathcal{Z}_0. \end{aligned} \quad (3.6)$$

In the derivation of flow equations for \mathcal{L} or Γ [see Eqs. (2.36) and (2.42)], we should keep in mind that in these functionals the fields Φ are held constant rather than the sources J . Hence, Eq. (2.36) implies

$$\partial_\Lambda \mathcal{L}[\Phi] = -\partial_\Lambda \mathcal{G}_c[J]|_{J=J_\Lambda[\Phi]}. \quad (3.7)$$

Using this and Eq. (3.6) we obtain for the functional $\Gamma[\Phi] = \mathcal{L}[\Phi] - S_0[\Phi]$,

$$\partial_\Lambda \Gamma = -\frac{1}{2} \text{Tr} \left(\partial_\Lambda [\mathbf{G}_0^{-1}] \left[\frac{\delta^{(2)} \mathcal{G}_c}{\delta J \delta J} \right]^T \right) + \partial_\Lambda \ln \mathcal{Z}_0. \quad (3.8)$$

To obtain a closed equation for Γ , we express the matrix $\frac{\delta^{(2)} \mathcal{G}_c}{\delta J \delta J}$ in terms of derivatives of Γ using Eq. (A4). After some rearrangements we obtain the exact flow equation for the generating functional $\Gamma[\Phi]$ of the one-line irreducible vertices

$$\begin{aligned} \partial_\Lambda \Gamma &= -\frac{1}{2} \text{Tr} \left[\mathbf{Z} \dot{\mathbf{G}}^T \mathbf{U}^T \left\{ \mathbf{1} - \mathbf{G}^T \mathbf{U}^T \right\}^{-1} \right] \\ &\quad -\frac{1}{2} \text{Tr} \left[\mathbf{Z} \dot{\mathbf{G}}_0^T \mathbf{\Sigma}^T \left\{ \mathbf{1} - \mathbf{G}_0^T \mathbf{\Sigma}^T \right\}^{-1} \right], \end{aligned} \quad (3.9)$$

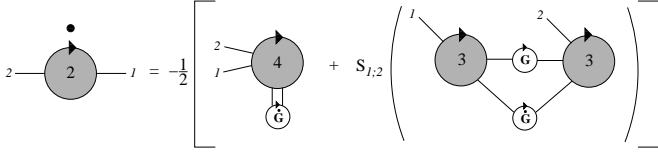


FIG. 2: Graphical representation of Eq. (3.16) for $n = 2$, describing the flow of the totally symmetric two-point vertex. Empty circles with \mathbf{G} and $\dot{\mathbf{G}}$ denote the exact matrix propagator \mathbf{G} and the single-scale propagator $\dot{\mathbf{G}}$ defined in Eqs. (2.24) and (3.10), respectively.

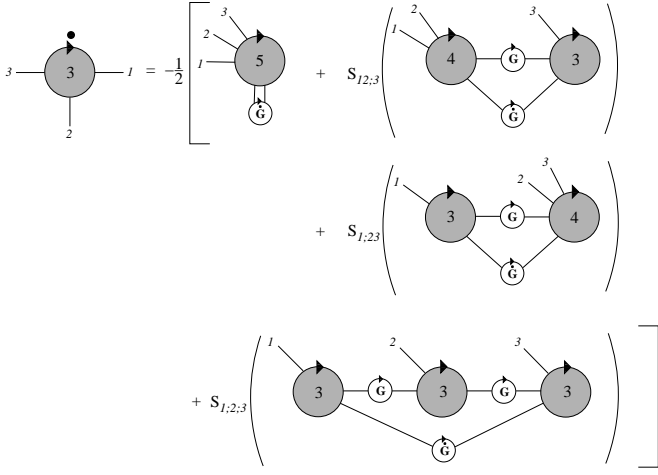


FIG. 3: Graphical representation of Eq. (3.16) for $n = 3$, describing the flow of the totally symmetric three-point vertex.

where the matrix $\mathbf{U}[\Phi]$ is the field-dependent part of the second functional derivative of $\Gamma[\Phi]$, as defined in Eq. (A1). For convenience we have defined the single scale propagator $\dot{\mathbf{G}}$ as

$$\dot{\mathbf{G}} = -\mathbf{G} \partial_\Lambda [\mathbf{G}_0^{-1}] \mathbf{G} = [\mathbf{1} - \mathbf{G}_0 \Sigma]^{-1} (\partial_\Lambda \mathbf{G}_0) [\mathbf{1} - \Sigma \mathbf{G}_0]^{-1}, \quad (3.10)$$

which reduces to $\dot{\mathbf{G}}_0 = \partial_\Lambda \mathbf{G}_0$ in the absence of interactions. The matrix $\dot{\mathbf{G}}$ has the same block-structure as the

matrix \mathbf{G} in Eq. (2.25). We denote the corresponding blocks by \dot{G} and \dot{F} . In the limit of a sharp Θ -function cutoff²⁸ the blocks of the single scale propagator are explicitly given by

$$[\dot{G}]_{K\sigma, K'\sigma'} = \delta_{K, K'} \delta_{\sigma\sigma'} \dot{G}_\sigma(K), \quad (3.11)$$

$$[\dot{F}]_{\bar{K}\sigma, \bar{K}'\sigma'} = \delta_{\bar{K} + \bar{K}', 0} \dot{F}_{\sigma\sigma'}(\bar{K}'), \quad (3.12)$$

with

$$\dot{G}_\sigma(K) = -\frac{\delta(\Lambda - D_K)}{i\omega - \xi_{\mathbf{k}\sigma} - \Sigma_\sigma(K)}, \quad (3.13)$$

$$\dot{F}_{\sigma\sigma'}(\bar{K}) = -\delta(\Lambda - \bar{D}_{\bar{K}}) [\hat{F}_0^{-1} + \hat{\Pi}]_{-\bar{K}\sigma, \bar{K}\sigma'}^{-1}, \quad (3.14)$$

where on the right-hand side of Eq. (3.14) it is understood that the Θ -function cutoff should be omitted from the matrix elements of \hat{F}_0 .

The second line in Eq. (3.9) does not depend on the fields any longer and therefore represents the flow of the interaction correction $\Gamma^{(0)}$ to the grand-canonical potential,

$$\partial_\Lambda \Gamma^{(0)} = -\frac{1}{2} \text{Tr} [\mathbf{Z} \dot{\mathbf{G}}_0^T \Sigma^T \{\mathbf{1} - \mathbf{G}_0^T \Sigma^T\}^{-1}]. \quad (3.15)$$

Since we have already dropped constant parts of the action in the Hubbard-Stratonovich transformation, we will not keep track of $\Gamma^{(0)}$ in the following either.

The first line on the right-hand side of Eq. (3.9) gives the flow of one-line irreducible vertices. We can generate a hierarchy of flow equations for the vertices by expanding both sides in powers of the fields. On the left-hand side, we simply insert the functional Taylor expansion (2.44) of $\Gamma[\Phi]$, while on the right-hand side we substitute the expansion of $\mathbf{U}[\Phi]$ given in Eq. (A7). For a comparison of the coefficients on both sides, the right-hand side has to be symmetrized with respect to external lines on different vertices. We can write down the resulting infinite system of flow equations for the one-line irreducible vertices $\Gamma^{(n)}$ with $n \geq 1$ in the following closed form,

$$\begin{aligned} \partial_\Lambda \Gamma_{\alpha_1, \dots, \alpha_n}^{(n)} = & -\frac{1}{2} \sum_{l=1}^{\infty} \sum_{m_1, \dots, m_l=1}^{\infty} \delta_{n, m_1 + \dots + m_l} \mathcal{S}_{\alpha_1, \dots, \alpha_{m_1}; \alpha_{m_1+1}, \dots, \alpha_{m_1+m_2}; \dots; \alpha_{m_1+\dots+m_{l-1}+1}, \dots, \alpha_n} \Big\{ \\ & \times \text{Tr} [\mathbf{Z} \dot{\mathbf{G}}^T \Gamma_{\alpha_1, \dots, \alpha_{m_1}}^{(m_1+2)T} \mathbf{G}^T \Gamma_{\alpha_{m_1+1}, \dots, \alpha_{m_1+m_2}}^{(m_2+2)T} \mathbf{G}^T \dots \Gamma_{\alpha_{m_1+\dots+m_{l-1}+1}, \dots, \alpha_n}^{(m_l+2)T}] \Big\}. \end{aligned} \quad (3.16)$$

Here the matrices $\Gamma_{\alpha_1 \dots \alpha_m}^{(m+2)}$ are given in Eq. (A8) and the symmetrization operator \mathcal{S} is defined in Eq. (A11). The effect of \mathcal{S} is rather simple: it acts on an expression already symmetric in the index groups separated by semi-

colons to generate an expression symmetric also with respect to the exchange of indices between different groups. From one summand in Eq. (3.16) the symmetrization operator \mathcal{S} thus creates $n!/(m_1! \dots m_l!)$ terms.

Figs. 2 and 3 show a graphical representation of the flow of the vertices $\Gamma^{(2)}$ and $\Gamma^{(3)}$. Note that with the graphical notation for the totally symmetric vertices introduced in Fig. 1 all the signs and combinatorics have a graphical representation. In the next subsection we will leave the shorthand notation and go back to more physical vertices, explicitly exhibiting the different types of fields. All this can be done on a graphical level and involves only straightforward combinatorics. In this sense the derivation of higher flow equations is at the same level of complexity as ordinary Feynman graph expansions.

C. Flow equations for physical vertices

Usually, the generating functional $\Gamma[\bar{\psi}, \psi, \varphi]$ is expanded in terms of correlation functions that are not symmetrized with respect to the exchange of legs involving different types of fields. If we explicitly display momentum and frequency conservation, such an expansion reads

$$\begin{aligned} \Gamma[\bar{\psi}, \psi, \varphi] = & \sum_{n=0}^{\infty} \sum_{m=0}^{\infty} \frac{1}{(n!)^2 m!} \int_{K'_1 \sigma'_1} \dots \int_{K'_n \sigma'_n} \int_{K_1 \sigma_1} \dots \int_{K_n \sigma_n} \int_{\bar{K}_1 \bar{\sigma}_1} \dots \int_{\bar{K}_m \bar{\sigma}_m} \delta_{K'_1 + \dots + K'_n, K_1 + \dots + K_n + \bar{K}_1 + \dots + \bar{K}_m} \\ & \times \Gamma^{(2n, m)}(K'_1 \sigma'_1, \dots, K'_n \sigma'_n; K_1 \sigma_1, \dots, K_n \sigma_n; \bar{K}_1 \bar{\sigma}_1, \dots, \bar{K}_m \bar{\sigma}_m) \\ & \times \bar{\psi}_{K'_1 \sigma'_1} \dots \bar{\psi}_{K'_n \sigma'_n} \psi_{K_1 \sigma_1} \dots \psi_{K_n \sigma_n} \varphi_{\bar{K}_1 \bar{\sigma}_1} \dots \varphi_{\bar{K}_m \bar{\sigma}_m}. \end{aligned} \quad (3.17)$$

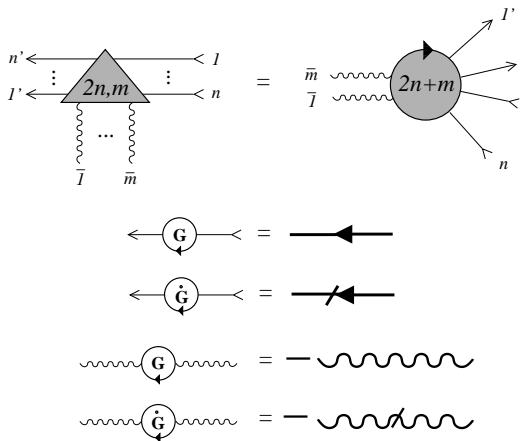


FIG. 4: Pictorial dictionary to translate graphs involving totally symmetrized vertices to ones involving physical vertices, which are only symmetrized within fields of the same type. The diagrams on the right hand sides of the last four lines represent G , \dot{G} , F and \dot{F} respectively.

Diagrammatically, we represent a physical vertex $\Gamma^{(2n, m)}$ involving $2n$ external fermion legs and m external boson legs by a triangle to emphasize that our theory contains three types of fields, see Fig. 4. We represent a leg associated with a $\bar{\psi}$ field by an arrow pointing outwards, a leg for ψ by an arrow pointing inwards, and a leg for φ with a wiggly line without an arrow. Recall that our Bose field is real because it couples to the density, so that it should be represented graphically by an undirected line. On the contrary, for a propagator G or \dot{G} , the field $\bar{\psi}$ is represented by an arrow pointing inwards and ψ by an arrow pointing outwards. Apart from the energy and

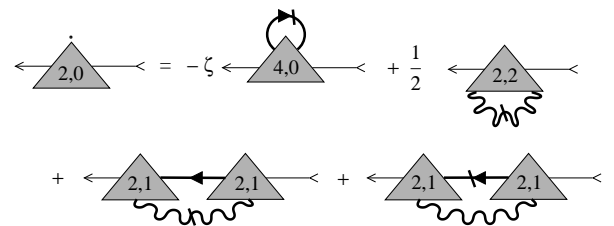


FIG. 5: Flow of the irreducible fermionic self-energy. The diagrams are obtained from the diagrams shown in Fig. 2 by specifying the external legs to be one outgoing and one incoming fermion leg.

momentum conserving delta-function, the totally symmetric vertices defined by the expansion (2.44) coincide with the non-symmetric ones in Eq. (3.17) for the same order of the indices. We can therefore obtain the flow equations for the non-symmetric vertices by choosing a definite realization of the external legs and by carrying out the intermediate sums over the different field species, i.e., by drawing all possible lines in the intermediate loop (two possible orientations of solid lines or a wiggly line). On the right-hand side one then has to appropriately order all the legs on the vertices keeping track of signs for the interchange of two neighboring fermion legs. Having done so, we can use the pictorial dictionary in Fig. 4 to obtain diagrams involving the physical correlation functions. In this way, we obtain from the diagram for the completely symmetric two-point vertex shown in Fig. 2 the diagram for the fermionic self-energy in Fig. 5 as well as the diagram for the irreducible polarization shown in Fig. 6. Moreover, if we specify the external legs in the diagram for the completely symmetric three-legged ver-

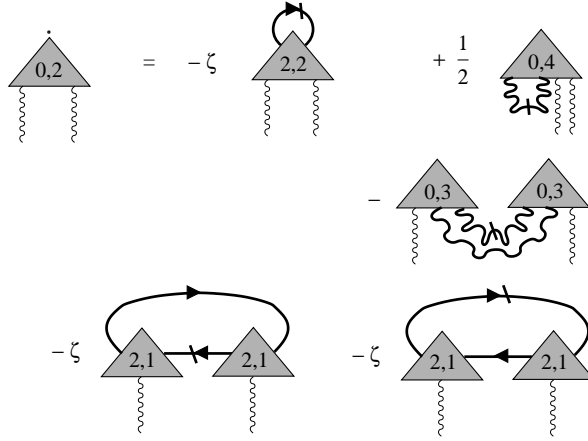


FIG. 6: Flow of the irreducible polarization, obtained from the totally symmetric diagram in Fig. 2 by setting both external legs equal to boson legs. Note that each closed fermion loop gives rise to an additional factor of $\zeta = -1$.

tex shown in Fig. 3 to be two fermion legs and one boson leg, we obtain the flow equation for the three-legged vertex shown in Fig. 7.

The flow equation for the vertex correction in Fig. 7 looks very complicated, so that at this point the reader might wonder how in one dimension we will be able to obtain the exact solution of the TLM using our approach. We shall explain this in detail in Sec. IV, but let us anticipate here the crucial step: obviously all diagrams shown in Figs. 5, 6, and 7 can be subdivided into two classes: those involving a fermionic single-scale propagator (the slash appears on a internal fermion line), and those with a bosonic single-scale propagator (with a slash on an internal boson line). At this point we have not specified the cutoff procedure, but in Sec. IV we shall work with a bosonic cutoff only. In this case all diagrams with a slash attached to a fermion line should simply be omitted. This is the crucial simplification which will allow us to solve the hierarchy of flow equations exactly. Let us proceed in this section without specifying a particular cutoff procedure.

D. Rescaling and classification of vertices

In order to assign scaling dimensions to the vertices, we have to define how we rescale momenta, frequencies and fields under the RG transformation. The rescaling is not unique but depends on the nature of the fixed point we are looking for. Let us be general here and assume that in the bosonic sector the relation between momentum and frequency is characterized by a bosonic dynamic exponent z_φ (this is the exponent z introduced by Hertz⁹) while in the fermionic sector the corresponding dynamic exponent is z_ψ . Rescaled dimensionless bosonic momenta

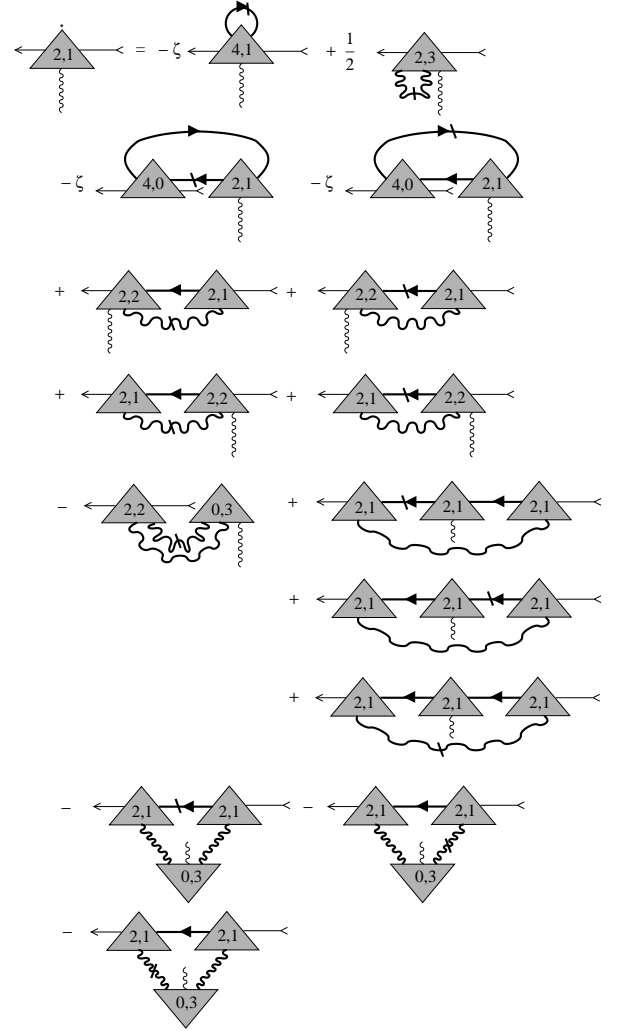


FIG. 7: Flow of three-legged vertex with two fermion leg and one boson leg, obtained as a special case of the diagram in Fig. 3.

$\bar{\mathbf{q}}$ and frequencies $\bar{\epsilon}$ are then introduced as usual⁹

$$\bar{\mathbf{q}} = \bar{\mathbf{k}}/\Lambda, \quad \bar{\epsilon} = \bar{\omega}/\bar{\Omega}_\Lambda, \quad \bar{\Omega}_\Lambda \propto \Lambda^{z_\varphi}. \quad (3.18)$$

The proper rescaling of the fermionic momenta is not so obvious. Certainly, all momenta should be measured with respect to suitable points \mathbf{k}_F on the Fermi surface. One possibility is to rescale only the component $k_{\parallel} = (\mathbf{k} - \mathbf{k}_F) \cdot \mathbf{v}_F$ of a given momentum that is parallel to the local Fermi velocity \mathbf{v}_F (and hence perpendicular to the Fermi surface).^{13,19} Unfortunately, in dimensions $D > 1$ this leads to rather complicated geometric constructions, because in a fixed reference frame the component of k_{\parallel} to be rescaled varies for different points on the Fermi surface. However, if the initial momentum transfer cutoff Λ_0 in Eq. (3.3) is small compared with the typical radius of the Fermi surface, the initial and final momenta associated with a scattering process lie both on nearby points on the Fermi surface. In this case it seems natural

to pick one fixed reference point $\mathbf{k}_{F,\sigma}$ on the Fermi surface, and then measure all fermionic momentum labels \mathbf{k}_i and \mathbf{k}'_i in $\Gamma^{(2n,m)}(K'_1, \dots, K'_n; K_1, \dots, K_n; \bar{K}_1, \dots, \bar{K}_m)$ relative to this $\mathbf{k}_{F,\sigma}$. Here, the index σ labels the different points on the Fermi surface, for example in one dimension $\alpha = \pm 1$, with $k_{F,\pm 1} = \pm k_F$. We then define rescaled fermionic momenta \mathbf{q} and frequencies ϵ as follows

$$\mathbf{q} = (\mathbf{k} - \mathbf{k}_{F,\sigma})/\Lambda, \quad \epsilon = \omega/\Omega_\Lambda, \quad \Omega_\Lambda \propto \Lambda^{z_\psi}. \quad (3.19)$$

Iterating the usual RG steps consisting of mode elimination and rescaling, we then coarse grain the degrees of freedom in a sphere around the chosen point $\mathbf{k}_{F,\sigma}$. Because by assumption the maximal momentum transfer mediated by the interaction is small compared with $|\mathbf{k}_{F,\sigma}|$, the fermionic momenta appearing in $\Gamma^{(2n,m)}(K'_1, \dots, K'_n; K_1, \dots, K_n; \bar{K}_1, \dots, \bar{K}_m)$ are all in the vicinity of the chosen $\mathbf{k}_{F,\sigma}$. This property is also responsible for the approximate validity of the *closed loop theorem* for interacting fermions with dominant forward scattering in arbitrary dimensions.^{44,45,46}

Apart from the rescaling of momenta and frequencies, we have to specify the rescaling of the fields. As usual, we require that the Gaussian part $S_0[\Phi] = S_0[\bar{\psi}, \psi] + S_0[\varphi]$ of our effective action is invariant under rescaling. For the fermionic part this is achieved by defining renormalized fields $\tilde{\psi}_{Q\sigma}$ in D dimensions via

$$\psi_{K\sigma} = \left(\frac{Z}{\Lambda^D \Omega_\Lambda^2} \right)^{1/2} \tilde{\psi}_{Q\sigma}, \quad (3.20)$$

where Z is the fermionic wave-function renormalization factor and $Q = (\mathbf{q}, i\epsilon)$ denotes the rescaled fermionic momenta and Matsubara frequencies as defined in Eq. (3.19). With this rescaling the wave-function renormalization and the Fermi velocity have a vanishing scaling dimension (corresponding to marginal couplings), while the momentum- and frequency independent part of the self-energy is relevant with scaling dimension +1, see Ref. 19. Analogously, we find that the bosonic Gaussian part of the action is invariant under rescaling if we express it in terms of the renormalized bosonic field $\tilde{\varphi}_{\bar{Q}\sigma}$ defined by

$$\varphi_{\bar{K}\sigma} = \left(\frac{\bar{Z}}{\Lambda^D \Omega_\Lambda \nu_0} \right)^{1/2} \tilde{\varphi}_{\bar{Q}\sigma}, \quad (3.21)$$

where \bar{Z} is the bosonic wave-function renormalization factor, $\bar{Q} = (\bar{\mathbf{q}}, i\bar{\epsilon})$ denotes the rescaled bosonic momenta

and Matsubara frequencies defined in Eq. (3.18), and ν_0 denotes the non-interacting density of states at the Fermi surface. We introduce the factor of ν_0 for convenience to make all rescaled vertices dimensionless. By construction Eq. (3.21) assigns vanishing scaling dimensions to the bare interaction parameters $f_{\mathbf{k}}^{\sigma\sigma'}$, corresponding to marginal Landau interaction parameters.

Expressing each term in the expansion of the generating functional $\Gamma[\bar{\psi}, \psi, \varphi]$ given in Eq. (3.17) in terms of the rescaled variables defined above and using the fact that Γ is dimensionless, we obtain the scaling form of the vertices. Omitting for simplicity the degeneracy labels σ , we define for $n \geq 1$ and $m \geq 1$, and for $z_\psi \leq z_\varphi$,⁵³

$$\begin{aligned} \tilde{\Gamma}_l^{(2n,m)}(Q'_1, \dots, Q'_n; Q_1, \dots, Q_n; \bar{Q}_1, \dots, \bar{Q}_m) = \\ \nu_0^{-m/2} \Lambda^{D(n-1+m/2)} \Omega_\Lambda^{-1} \bar{\Omega}_\Lambda^{m/2} Z^n \bar{Z}^{m/2} \\ \times \Gamma_\Lambda^{(2n,m)}(K'_1, \dots, K'_n; K_1, \dots, K_n; \bar{K}_1, \dots, \bar{K}_m). \end{aligned} \quad (3.22)$$

In the case of purely bosonic vertices ($n = 0$) we set

$$\begin{aligned} \tilde{\Gamma}_l^{(0,m)}(\bar{Q}_1, \dots, \bar{Q}_m) = \nu_0^{-m/2} (\Lambda^D \bar{\Omega}_\Lambda)^{-1+m/2} \bar{Z}^{m/2} \\ \times \Gamma_\Lambda^{(0,m)}(\bar{K}_1, \dots, \bar{K}_m), \end{aligned} \quad (3.23)$$

while for the fermionic two-point vertex (i.e., the rescaled irreducible self-energy, corresponding to $n = 1$ and $m = 0$) we should subtract the exact fixed point self-energy $\Sigma_*(\mathbf{k}_{F,\sigma}, i0)$ at the Fermi-surface reference-point $\mathbf{k}_{F,\sigma}$ and for vanishing frequency as a counter-term,^{19,21}

$$\tilde{\Gamma}_l^{(2,0)}(Q; Q) \equiv \tilde{\Sigma}_l(Q) = \frac{Z}{\Omega_\Lambda} [\Sigma(K) - \Sigma_*(\mathbf{k}_{F,\sigma}, i0)]. \quad (3.24)$$

If necessary, the counter-term $\Sigma_*(\mathbf{k}_{F,\sigma}, i0)$ can be reconstructed from the condition that the constant part $\tilde{r}_l = \tilde{\Sigma}_l(0)$ of the self-energy flows into an RG fixed point.^{19,21} We consider the rescaled vertices to be functions of the logarithmic flow parameter $l = -\ln(\Lambda/\Lambda_0)$. Introducing the flowing anomalous dimensions associated with the fermionic and bosonic fields,

$$\eta_l = -\partial_l \ln Z, \quad \bar{\eta}_l = -\partial_l \ln \bar{Z}, \quad (3.25)$$

we can then write down the flow equations for the rescaled vertices. Omitting the arguments, we obtain for $n \geq 1$ the flow equation⁵³

$$\partial_l \tilde{\Gamma}_l^{(2n,m)} = \left[(1-n)D + z_{\min} - \frac{m}{2}(D + z_\varphi) - n\eta_l - \frac{m}{2}\bar{\eta}_l - \sum_{i=1}^n (Q'_i \cdot \frac{\partial}{\partial Q'_i} + Q_i \cdot \frac{\partial}{\partial Q_i}) - \sum_{i=1}^m \bar{Q}_i \cdot \frac{\partial}{\partial \bar{Q}_i} \right] \tilde{\Gamma}_l^{(2n,m)} + \dot{\tilde{\Gamma}}_l^{(2n,m)}, \quad (3.26)$$

where $z_{\min} = \min\{z_\varphi, z_\psi\}$. For $n = 0$ we obtain from Eq. (3.23)

$$\partial_l \tilde{\Gamma}_l^{(0,m)} = \left[(1 - \frac{m}{2})(D + z_\varphi) - \frac{m}{2} \bar{\eta}_l - \sum_{i=1}^m \bar{Q}_i \cdot \frac{\partial}{\partial \bar{Q}_i} \right] \tilde{\Gamma}_l^{(0,m)} + \dot{\tilde{\Gamma}}_l^{(0,m)}, \quad (3.27)$$

where we have introduced the notation

$$\mathbf{Q} \cdot \frac{\partial}{\partial \mathbf{Q}} = \mathbf{q} \cdot \nabla_{\mathbf{q}} + z_\psi \epsilon \frac{\partial}{\partial \epsilon}, \quad (3.28)$$

$$\bar{\mathbf{Q}} \cdot \frac{\partial}{\partial \bar{\mathbf{Q}}} = \bar{\mathbf{q}} \cdot \nabla_{\bar{\mathbf{q}}} + z_\varphi \bar{\epsilon} \frac{\partial}{\partial \bar{\epsilon}}. \quad (3.29)$$

The inhomogeneities in Eqs. (3.26) and (3.27) are given by the rescaled version of the right-hand sides of the flow equations for the unrescaled vertices, i.e., for $n \geq 1$, and $z_\psi \leq z_\varphi$,⁵³

$$\begin{aligned} \dot{\tilde{\Gamma}}_l^{(2n,m)}(Q'_1, \dots, Q'_n; Q_1, \dots, Q'_n; \bar{Q}_1, \dots, \bar{Q}_m) = \\ \nu_0^{-m/2} \Lambda^{D(n-1+m/2)} \Omega_\Lambda^{-1} \bar{\Omega}_\Lambda^{m/2} Z^n \bar{Z}^{m/2} \\ \times [-\Lambda \partial_\Lambda \Gamma_\Lambda^{(2n,m)}(\{K'_i; K_i; \bar{K}_i\})], \end{aligned} \quad (3.30)$$

and for $n = 0$,

$$\begin{aligned} \dot{\tilde{\Gamma}}_l^{(0,m)}(\bar{Q}_1, \dots, \bar{Q}_m) = \nu_0^{-m/2} (\Lambda^D \bar{\Omega}_\Lambda)^{-1+m/2} \bar{Z}^{m/2} \\ \times [-\Lambda \partial_\Lambda \Gamma_\Lambda^{(0,m)}(\bar{K}_1, \dots, \bar{K}_m)]. \end{aligned} \quad (3.31)$$

By properly counting all factors it is then not difficult to see that the explicit expressions for the inhomogeneities in Eqs. (3.30) and (3.31) can be simply obtained from their unrescaled counter-parts by replacing all vertices and propagators with their rescaled analogues, where the rescaled propagators are defined by

$$G(K) = \frac{Z}{\Omega_\Lambda} \tilde{G}(Q), \quad F(\bar{K}) = \frac{\bar{Z}}{\nu_0} \tilde{F}(\bar{Q}), \quad (3.32)$$

and the corresponding rescaled single scale propagators are defined via

$$\Lambda \dot{G}(K) = -\frac{Z}{\Omega_\Lambda} \dot{\tilde{G}}(Q), \quad \Lambda \dot{F}(\bar{K}) = -\frac{\bar{Z}}{\nu_0} \dot{\tilde{F}}(\bar{Q}) \quad (3.33)$$

From Eqs. (3.26) and (3.27) we can read off the scaling dimensions of the vertices: the scaling dimension of $\tilde{\Gamma}^{(2n,m)}$ in D dimensions is

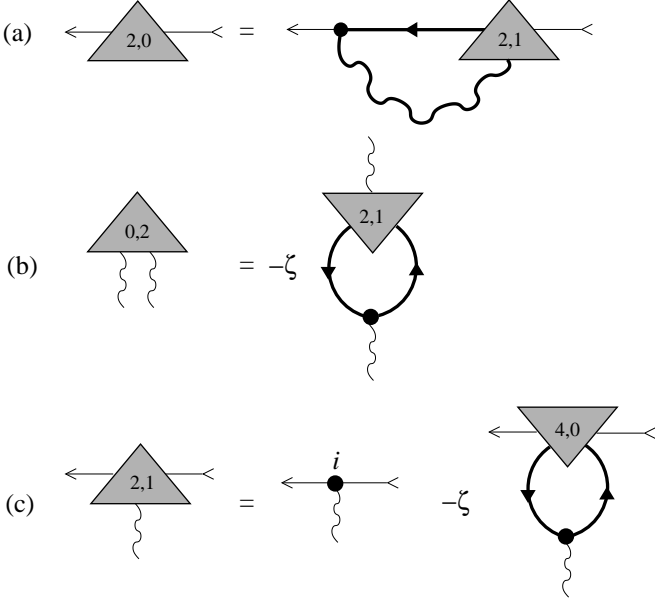
$$D^{(2n,m)} = \begin{cases} (1-n)D + z_{\min} - (D+z_\varphi)m/2 & \text{for } n \geq 1 \\ (D+z_\varphi)(1-m/2) & \text{for } n = 0 \end{cases} \quad (3.34)$$

In the particular case of the Tomonaga-Luttinger model, where $D = 1$ and $z_\psi = z_\varphi = 1$, we have $D^{(2n,m)} = 2 - n - m$. Hence, in this case $\tilde{\Gamma}^{(2,0)}(Q = 0)$ and $\tilde{\Gamma}^{(0,1)}$ are relevant with scaling dimension +1, $\tilde{\Gamma}^{(4,0)}(Q_i = 0)$ and $\tilde{\Gamma}^{(2,1)}(Q_i = \bar{Q}_i = 0)$ are marginal. All other vertices are irrelevant. Of course, the linear terms in the expansion of $\tilde{\Gamma}^{(2,0)}(Q; Q)$ for small Q are also marginal.

These terms determine the wave-function renormalization factor Z and the Fermi velocity renormalization \tilde{v}_l , see Eqs. (4.20) and (4.24) below. Note that for short-range interactions the dispersion of the zero-sound mode is linear in any dimension.⁴⁵ Hence, as long as the density response is dominated by the zero sound mode, Eq. (3.34) remains valid for $D > 1$ with $z_\psi = z_\varphi = 1$. In this case the scaling dimension of the purely fermionic four-point vertex is $D^{(4,0)} = 1 - D$ and the scaling dimension of the three-legged vertex with two fermion legs and one boson leg is $D^{(2,1)} = (1 - D)/2$. Note that both vertices become irrelevant in $D > 1$. As discussed in the following subsection, this means that the random-phase approximation (RPA) for the effective interaction, as well as the so-called GW-approximation⁵⁴ for the fermionic self-energy, are qualitatively correct in $D > 1$.

E. A simple truncation scheme: keeping only the skeleton elements for two-point functions

In order to solve the flow equations explicitly, one is forced to truncate the infinite hierarchy of flow equations. In the one-particle irreducible version of the purely fermionic functional RG it is common practice^{14,15,16,17,25,26} to retain only vertices up to the four-point vertex and set all higher order vertices equal to zero. Our approach offers new possibilities for truncation schemes. Consider the skeleton graphs³³ for the one-particle irreducible fermionic self-energy and the one-interaction-line irreducible polarization shown in Fig. 8 (a) and (b). The skeleton graphs contain three basic elements: the exact fermionic Green function, the exact bosonic Green function (i.e., the effective screened interaction), and the three-legged vertex with two fermion legs and one boson leg. A systematic derivation of the skeleton expansion for the vertices in our coupled Fermi-Bose theory is presented in Appendix B. One advantage of our RG approach (as compared with more conventional methods involving only fermionic fields) is that it yields directly the flow equations for basic elements appearing in the skeleton graphs for the self-energy and the polarization shown in Fig. 8. Of course, in principle the three-legged vertex can be obtained from the vertex with four fermion legs with the help of the skeleton graph shown in Fig. 8 (c). However, calculating the three-legged vertex from the four-legged vertex in this way involves an intermediate integration, which requires the knowledge of the momentum and frequency dependence of the four-legged vertex. Unfortunately, in practice the purely fermionic functional RG equations have to be severely truncated



so that up to now it has not been possible to keep track of the frequency-dependence of the four-legged fermion vertex within the purely fermionic functional RG.

To obtain a closed system of RG equations involving only the skeleton elements, let us retain only the vertices $\Sigma_\sigma(K)$, $\Pi_\sigma(\bar{K})$ and $\Gamma^{(2,1)}(K + \bar{K}\sigma; K\sigma; \bar{K}\sigma)$ on the right-hand sides of the exact flow equations for these quantities shown in Figs. 5, 6, and 7, and set all other vertices equal to zero. The resulting closed system of flow equations is shown graphically in Fig. 9. Explicitly, the flow equations are

$$\begin{aligned} \partial_\Lambda \Sigma_\sigma(K) = & \\ & \int_{\bar{K}} \left[\dot{F}_{\sigma\sigma}(\bar{K}) G_\sigma(K + \bar{K}) + F_{\sigma\sigma}(\bar{K}) \dot{G}_\sigma(K + \bar{K}) \right] \\ & \times \Gamma^{(2,1)}(K + \bar{K}\sigma; K\sigma; \bar{K}\sigma) \Gamma^{(2,1)}(K\sigma; K + \bar{K}\sigma; -\bar{K}\sigma) , \end{aligned} \quad (3.35)$$

$$\begin{aligned} \partial_\Lambda \Pi_\sigma(\bar{K}) = & \\ & -\zeta \int_K \left[\dot{G}_\sigma(K) G_\sigma(K + \bar{K}) + G_\sigma(K) \dot{G}_\sigma(K + \bar{K}) \right] \\ & \times \Gamma^{(2,1)}(K + \bar{K}\sigma; K\sigma; \bar{K}\sigma) \Gamma^{(2,1)}(K\sigma; K + \bar{K}\sigma; -\bar{K}\sigma) , \end{aligned} \quad (3.36)$$

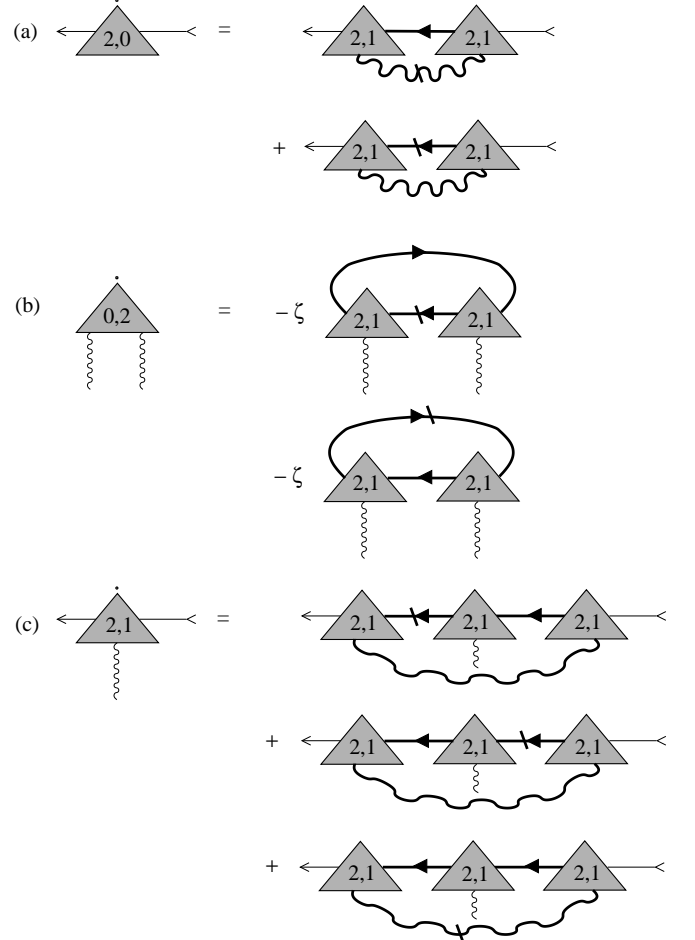


FIG. 9: Truncation of the flow equations for (a) fermionic self-energy, (b) irreducible polarization, and (c) three-legged vertex which sets all other vertices equal to zero. Note that the internal lines are full propagators, which depend on the self-energies $\Gamma^{(2,0)} = \Sigma$ and $\Gamma^{(0,2)} = \Pi$.

$$\begin{aligned} \partial_\Lambda \Gamma^{(2,1)}(K + \bar{K}\sigma; K\sigma; \bar{K}\sigma) = & \\ & \int_{\bar{K}'} \left[\dot{F}_{\sigma\sigma}(\bar{K}') G_\sigma(K + \bar{K}') G_\sigma(K + \bar{K} + \bar{K}') \right. \\ & + F_{\sigma\sigma}(\bar{K}') \dot{G}_\sigma(K + \bar{K}') G_\sigma(K + \bar{K} + \bar{K}') \\ & + F_{\sigma\sigma}(\bar{K}') G_\sigma(K + \bar{K}') \dot{G}_\sigma(K + \bar{K} + \bar{K}') \left. \right] \\ & \times \Gamma^{(2,1)}(K + \bar{K}\sigma; K + \bar{K} + \bar{K}'\sigma; -\bar{K}'\sigma) \\ & \times \Gamma^{(2,1)}(K + \bar{K} + \bar{K}'\sigma; K + \bar{K}'\sigma; \bar{K}\sigma) \\ & \times \Gamma^{(2,1)}(K + \bar{K}'\sigma; K\sigma; \bar{K}'\sigma) . \end{aligned} \quad (3.37)$$

These equations form a closed system of integro-differential equations that can in principle be solved numerically. If the initial momentum transfer cutoff Λ_0 is chosen larger than the maximal momentum transferred by the bare interaction, and the initial bandwidth cut-off $v_0\Lambda_0$ is larger than the bandwidth of the bare energy dispersion, then the initial conditions are $\Sigma_\sigma(K)_{\Lambda_0} = 0$, $\Pi_\sigma(\bar{K})_{\Lambda_0} = 0$, and $\Gamma^{(2,1)}(K + \bar{K}\sigma; K\sigma; \bar{K}\sigma)_{\Lambda_0} = i$. A nu-

merical solution of these coupled equations seems to be a formidable task, which we shall not attempt in this work. Note, however, that in Sec. III D we have argued that for regular interactions in dimensions $D > 1$ the three-legged vertex is actually irrelevant in the RG sense. Hence, we expect that the qualitatively correct behavior of the fermionic self-energy and the polarization can be obtained by ignoring the flow of the three-legged vertex, setting $\Gamma^{(2,1)} \rightarrow i$. If we further ignore interaction corrections to the internal propagators in the flow equation (3.36) for the polarization, it is easy to see that the solution of this equation is nothing but the non-interacting polarization. This is equivalent with the RPA for the effective interaction. Substituting this into the flow equation (3.35) for the self-energy and ignoring again self-energy corrections to the internal Green functions, we obtain the non self-consistent GW approximation⁵⁴ for the fermionic self-energy. For regular interactions in $D > 1$ we therefore expect that the RPA and the GW approximation are qualitatively correct. However, for strong bare interactions quantitatively accurate results can only be expected if the vertex corrections described by Eq. (3.37) are at least approximately taken into account.

We shall consider this problem again in Sec. IV D, where we discuss truncations of an expansion based on relevance. To lowest order, this approximation will agree with Eqs. (3.35–3.37) when the dependence of the vertex $\Gamma^{(2,1)}$ on momenta and frequencies is ignored. There, we use the resulting equations to calculate an approximation to the electronic Green function of the one-dimensional Tomonaga-Luttinger model. Amazingly, this simple truncation is sufficient to reproduce the correct anomalous dimension known from bosonization.

IV. THE MOMENTUM-TRANSFER CUTOFF AS FLOW PARAMETER

The truncation discussed in Sec. III E violates the Ward identities relating vertices with different numbers of external legs (for a self-contained derivation of the Ward identities within the framework of our functional integral approach, see App. C). Moreover, even if we do not truncate the exact hierarchy of flow equations shown in Figs. 5, 6, and 7, the Ward identities are violated for any finite value of the bandwidth-cutoff $v_0\Lambda$, because the cutoff leads to a violation of the underlying gauge symmetry. We can thus only expect the Ward identities to be restored in the limit $v_0\Lambda \rightarrow 0$. Recall that in the TLM the Ward identities are valid in the strict sense only in the presence of the Dirac-sea implying that the ultraviolet cutoff $v_0\Lambda_0$ has been removed. The Ward identities and the underlying asymptotic conservation laws are crucial for the exact solubility of the Tomonaga-Luttinger model^{42,43} and its higher-dimensional generalization.^{44,45} In order to reproduce the exact solution of the TLM known from bosonization within the functional RG, it

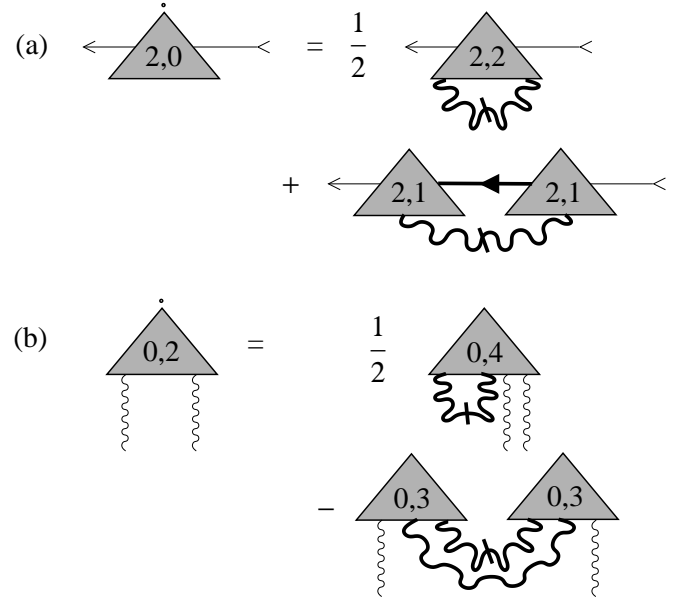


FIG. 10: Exact flow equations for (a) the fermionic self-energy and (b) the irreducible polarization in the momentum transfer cutoff scheme.

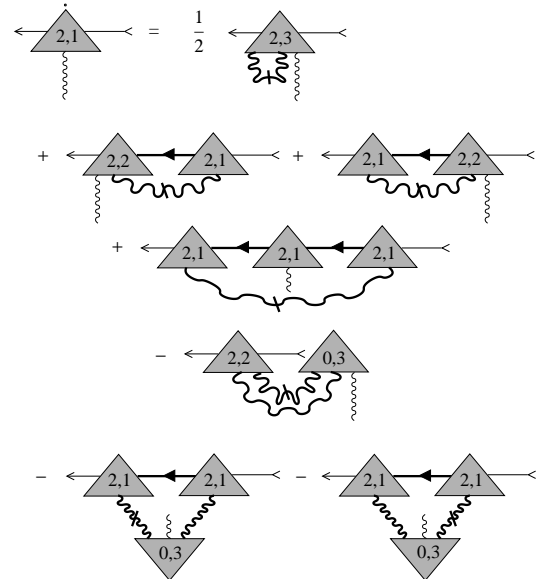


FIG. 11: Exact flow equations for the three-legged vertex with two fermion legs and one boson leg in the momentum transfer cutoff scheme.

is very important to have RG flow equations which are consistent with the Ward identities even for finite values of the cutoff. In this section we show that this requirement is fulfilled if we work in our mixed Fermi-Bose RG with a momentum transfer cutoff Λ only and take the limit $v_0\Lambda \rightarrow 0$ of a vanishing bandwidth cutoff.

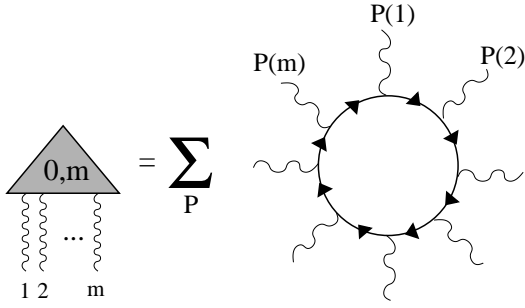


FIG. 12: Initial condition for the pure boson vertices in the momentum transfer cutoff scheme. The sum is taken over the $m!$ permutations of the labels of the external legs. For linearized energy dispersion all symmetrized closed fermion loops with more than two external legs vanish.

A. Exact flow equations for momentum-transfer cutoff

As already briefly mentioned at the end of Sec. III C, if we work with a momentum transfer cutoff Λ only, then all diagrams with a slash on an internal fermionic Green function [corresponding to the fermionic component of the single scale propagator given in Eq. (3.13)] on the right-hand sides of the exact flow equations shown in Figs. 5, 6, and 7 should be omitted. The exact flow equations for the electronic self-energy and the irreducible polarization then become

$$\begin{aligned} \partial_\Lambda \Sigma_\sigma(K) = & \frac{1}{2} \int_{\bar{K}} \dot{F}_{\sigma\sigma}(\bar{K}) \Gamma^{(2,2)}(K\sigma; K\sigma; \bar{K}\sigma, -\bar{K}\sigma) \\ & + \int_{\bar{K}} \dot{F}_{\sigma\sigma}(\bar{K}) G_\sigma(K + \bar{K}) \Gamma^{(2,1)}(K + \bar{K}\sigma; K\sigma; \bar{K}\sigma) \\ & \times \Gamma^{(2,1)}(K\sigma; K + \bar{K}\sigma; -\bar{K}\sigma), \end{aligned} \quad (4.1)$$

$$\begin{aligned} \partial_\Lambda \Pi_\sigma(\bar{K}) = & \frac{1}{2} \int_{\bar{K}'} \dot{F}_{\sigma\sigma}(\bar{K}) \Gamma^{(0,4)}(\bar{K}'\sigma, -\bar{K}'\sigma, \bar{K}\sigma, -\bar{K}\sigma) \\ & - \int_{\bar{K}'} \dot{F}_{\sigma\sigma}(\bar{K}') F_{\sigma\sigma}(\bar{K} + \bar{K}') \Gamma^{(0,3)}(-\bar{K}\sigma, \bar{K} + \bar{K}'\sigma, -\bar{K}'\sigma) \\ & \times \Gamma^{(0,3)}(\bar{K}'\sigma, -\bar{K} - \bar{K}'\sigma, \bar{K}\sigma). \end{aligned} \quad (4.2)$$

These equations are shown graphically in Fig. 10. A graphical representation of the corresponding exact flow equation for the three-legged vertex is shown in Fig. 11. Still, these flow equations look rather complicated. Since we have imposed a cutoff only in the momentum transferred by the bosons, the initial conditions at scale Λ_0 are non-trivial. The initial value of the three-legged vertex is still $\Gamma_{\Lambda_0}^{(2,1)} = i$, but the pure boson vertices $\Gamma^{(0,m)}$ with m external legs are initially given by the symmetrized closed

fermion loops shown in Fig. 12. All other vertices vanish at the initial scale Λ_0 . An essential simplification occurs now if we linearize the energy dispersion relative to the Fermi surface. If the initial momentum transfer cutoff Λ_0 is small compared with the typical Fermi momentum, then we may set all pure boson vertices $\Gamma^{(0,m)}$ with more than two external boson legs ($m \geq 2$) equal to zero. This is nothing but the closed loop theorem,^{42,43,44,45,46} which is valid exactly for the one-dimensional TLM (where the energy dispersion is linear by definition). In higher dimensions, the closed loop theorem is valid to a very good approximation as long as the linearization of the energy dispersion is justified within a given sectorization of the Fermi surface and scattering processes that transfer momentum between different sectors of the Fermi surface can be neglected.^{45,46} Note that the closed loop theorem is consistent with the momentum transfer cutoff flow, because pure boson vertices $\Gamma^{(0,m)}$ with $m \geq 3$ are not generated if they initially vanish.

Assuming the validity of the closed loop theorem, the right-hand side of the flow equation (4.2) for the polarization vanishes identically, because it depends only on boson vertices with more than two external legs. Physically, this means that there are no corrections to the non-interacting polarization, so that the RPA for the effective interaction is exact. This is of course well known since the pioneering work by Dzyaloshinskii and Larkin.⁴² Moreover, the last three diagrams in the flow equation for $\Gamma^{(2,1)}$ shown in Fig. 11 also vanish, because they contain the vertex $\Gamma^{(0,3)}$. However, the remaining diagrams in Fig. 10 (a) and Fig. 11 still look quite complicated, so that we still have to solve an infinite hierarchy of coupled flow equations. In the next subsection we show how this infinite system of coupled integro-differential equations can be solved exactly.

B. Ward identities as solutions of the infinite hierarchy of flow equations

Let us consider the terms on the right-hand sides of the flow equations for the vertices $\Gamma^{(2,m)}$ with two external fermion legs and an arbitrary number of boson legs assuming the validity of the closed loop theorem, so that all pure boson vertices $\Gamma^{(0,m)}$ with $m \geq 2$ vanish. From Fig. 10 (a) and Fig. 11 it is clear that in general the right-hand side of the flow equation for $\partial_\Lambda \Gamma^{(2,m)}$ depends on $\Gamma^{(2,m+2)}$ and on all $\Gamma^{(2,m')}$ with $m' \leq m$. In fact, from our general expression for the flow of the totally symmetrized vertices given in Eq. (3.16) we can derive the flow equations for the vertices $\Gamma^{(2,m)}$ with arbitrary m in closed form (we omit for simplicity the degeneracy index σ),

$$\begin{aligned}
\partial_\Lambda \Gamma^{(2,m)}(K'; K; \bar{K}_1, \dots, \bar{K}_m) &= \frac{1}{2} \int_{\bar{K}} \dot{F}_{\sigma\sigma}(\bar{K}) \Gamma^{(2,m+2)}(K'; K; -\bar{K}, \bar{K}, \bar{K}_1, \dots, \bar{K}_m) + \sum_{l=2}^{\infty} \sum_{m_1, \dots, m_l=1}^{\infty} \delta_{m, \sum_i m_i} \left[\prod_i m_i! \right]^{-1} \\
&\times \sum_P \int_{\bar{K}} \dot{F}(\bar{K}) \Gamma^{(2,m_1+1)}(K'; \tilde{K}_1; \bar{K}_{P(1)}, \dots, \bar{K}_{P(m_1), -\bar{K}}) G(\tilde{K}_1) \Gamma^{(2,m_2)}(\tilde{K}_1; \tilde{K}_2; \bar{K}_{P(m_1+1)}, \dots, \bar{K}_{P(m_1+m_2)}) \\
&\times G(\tilde{K}_2) \cdot \dots \cdot G(\tilde{K}_{l-1}) \Gamma^{(2,m_l+1)}(\tilde{K}_{l-1}; K; \bar{K}, \bar{K}_{P(m-m_l+1)}, \dots, \bar{K}_{P(m)}) , \tag{4.3}
\end{aligned}$$

where we have defined

$$K' = K + \sum_{i=1}^m \bar{K}_i, \quad \tilde{K}_i = K' + \bar{K} - \sum_{j=1}^{m_1+...+m_i} \bar{K}_{P(j)}, \tag{4.4}$$

and P denotes a permutation of $\{1, \dots, m\}$. A graphical representation of Eq. (4.3) is shown in Fig. 13. Note that the flow equation (4.1) for the irreducible self-energy is a special case of Eq. (4.3) for $m = 0$.

We are now facing the problem of solving the infinite hierarchy of coupled flow equations given by Eq. (4.3). In view of the fact that these equations are exact and that in one dimension the single-particle Green function of the TLM can be calculated exactly via bosonization, we expect that this infinite hierarchy of flow equations can also be solved exactly. Indeed, the solutions of these equations are nothing but infinitely many Ward identities relating the vertex $\Gamma^{(2,m)}$ with two fermion legs and m boson legs to the vertex $\Gamma^{(2,m-1)}$ with one boson leg less.

We derive these Ward identities within the framework of our functional integral approach in Appendix C. For $m = 1$ the Ward identity is well known^{42,43,44,45}

$$\begin{aligned}
G(K + \bar{K}) \Gamma^{(2,1)}(K + \bar{K}; K; \bar{K}) G(K) &= \\
&= \frac{-i}{i\bar{\omega} - \mathbf{v}_{F,\sigma} \cdot \bar{\mathbf{k}}} [G(K + \bar{K}) - G(K)] . \tag{4.5}
\end{aligned}$$

Here $\mathbf{v}_{F,\sigma}$ is the Fermi velocity associated with the independent fermionic label $K = (\mathbf{k}, i\omega)$, where $|\mathbf{k} - \mathbf{k}_{F,\sigma}| \ll |\mathbf{k}_{F,\sigma}|$. Note that the Ward identity (4.5) has been used in Refs. 42 and 44 to close the skeleton equation for the self-energy and thus obtain the exact Green function of the TLM without invoking the machinery of bosonization. However, for solving the TLM exactly within the framework of the functional RG, we also need the Ward identities for the vertices $\Gamma^{(2,m)}$ with $m \geq 1$. As shown in Appendix C, for linear energy dispersion we have

$$\begin{aligned}
\Gamma^{(2,m)}(K'; K; \bar{K}_1, \dots, \bar{K}_m) &= \frac{-i}{i\bar{\omega}_l - \mathbf{v}_{F,\sigma} \cdot \bar{\mathbf{k}}_l} \left[\Gamma^{(2,m-1)}(K'; K + \bar{K}_l; \bar{K}_1, \dots, \bar{K}_{l-1}, \bar{K}_{l+1}, \dots, \bar{K}_m) \right. \\
&\quad \left. - \Gamma^{(2,m-1)}(K' - \bar{K}_l; K; \bar{K}_1, \dots, \bar{K}_{l-1}, \bar{K}_{l+1}, \dots, \bar{K}_m) \right] , \tag{4.6}
\end{aligned}$$

where $1 \leq l \leq m$. For clarity let us write down here the special case $m = 2$,

$$\begin{aligned}
\Gamma^{(2,2)}(K + \bar{K}_1 + \bar{K}_2; K; \bar{K}_1, \bar{K}_2) &= \frac{-i}{i\bar{\omega}_1 - \mathbf{v}_{F,\sigma} \cdot \bar{\mathbf{k}}_1} \left[\Gamma^{(2,1)}(K + \bar{K}_1 + \bar{K}_2; K + \bar{K}_1; \bar{K}_2) - \Gamma^{(2,1)}(K + \bar{K}_2; K; \bar{K}_1) \right] \\
&= \frac{-i}{i\bar{\omega}_2 - \mathbf{v}_{F,\sigma} \cdot \bar{\mathbf{k}}_2} \left[\Gamma^{(2,1)}(K + \bar{K}_1 + \bar{K}_2; K + \bar{K}_2; \bar{K}_1) - \Gamma^{(2,1)}(K + \bar{K}_1; K; \bar{K}_1) \right] . \tag{4.7}
\end{aligned}$$

Diagrammatic representations of the Ward identities given in Eqs. (4.5) and (4.6) are shown in Fig. 14. To proof that these Ward identities indeed solve our infinite system of flow equations given by Eqs. (4.1) and (4.3), we start from the flow equation for $\Gamma^{(2,m+1)}$. Substituting on both sides of this exact flow equation the Ward identities, we can reduce it to a new flow equation in-

volving only vertices where the number of boson legs is reduced by one, but with an external bosonic momentum entering the vertices at various places. Graphically, we indicate the place where the bosonic momentum enters the vertex by a double-slash, as shown in Fig. 14. The important point is now that all diagrams with double-slashes attached to intermediate Green functions cancel

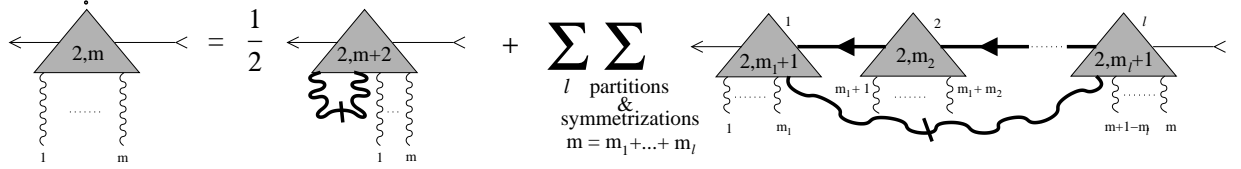


FIG. 13: Diagrammatic representation of the flow equation (4.3) of vertices with two fermion legs and a general number of boson legs provided the pure boson vertices with more than two external legs vanish, as implied by the closed loop theorem.

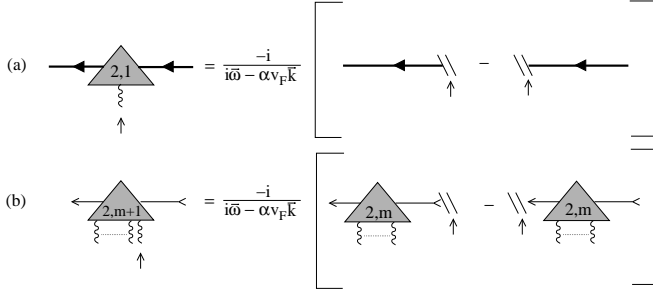


FIG. 14: (a) Diagrammatic representation of the Ward identity (4.5) for the three-legged vertex and (b) of the Ward identity (4.6) for the vertex with two fermion legs and $m > 1$ boson legs. The small arrow indicates the place in the diagram where the external bosonic energy-momentum enters. A double-slash to the right of an arrow means that the bosonic momentum is added before the corresponding Green function, while a double-slash to the left of an arrow means that the momentum is added after the Green function.

due to the fact that all vertices $\Gamma^{(2,m)}$ can be expressed in terms of a difference of vertices $\Gamma^{(2,m-1)}$, with a same prefactor that is independent of m . Graphically, only the diagrams with a double-slash attached to the leftmost or rightmost Green function survive. Canceling the common prefactor, it is then easy to see that the RG equation derived in this way from the functional RG equation for $\Gamma^{(2,m+1)}$ is nothing but the exact RG equation for $\Gamma^{(2,m)}$. Hence, the Ward identities provide relations between the vertices $\Gamma^{(2,m)}$ which are consistent with the relations implied by the exact hierarchy of RG flow equations in the momentum transfer cutoff scheme. In other words, the Ward identities are the solutions of the infinite hierarchy of flow equations!

C. Exact solution of the Tomonaga-Luttinger model via the exact RG

Given the cascade of Ward identities (4.5) and (4.6) we can close the integro-differential equation (4.1) for the irreducible self-energy. Note that this equation involves both the three-legged vertex and the four-legged vertex with two fermion legs and two boson legs, so that the Ward identity (4.5) is not sufficient to close the flow equation. Of course, if one is only interested in calculating the Green function of the TLM, it is simpler to start

from the skeleton equation for the self-energy shown in Fig. 8, which can be closed by means of the Ward identity (4.5) for the three-legged vertex only. Nevertheless, it is instructive to see how the exact solution emerges within the framework of the functional RG. Substituting Eqs. (4.5) and (4.7) into Eq. (4.1), we obtain the following integro-differential equation for the electronic self-energy,

$$\partial_\Lambda \Sigma_\sigma(K) = G_\sigma^{-2}(K) \int_{\bar{K}} \frac{\dot{F}_{\sigma\sigma}(\bar{K})}{(i\bar{\omega} - \mathbf{v}_{F,\sigma} \cdot \bar{\mathbf{k}})^2} \times [G_\sigma(K) - G_\sigma(K + \bar{K})]. \quad (4.8)$$

Here the index σ labels not only the different spin species, but also the different patches of the sectorized Fermi surface.⁴⁵ For example, for the spin-less case $\sigma = \pm k_F$. Using the fact that in the momentum-transfer cutoff scheme $G^2 \partial_\Lambda \Sigma = \partial_\Lambda G$ we can alternatively write Eq. (4.8) as a *linear* integro-differential equation for the fermionic Green function,

$$\partial_\Lambda G_\sigma(K) = \int_{\bar{K}} \frac{\dot{F}_{\sigma\sigma}(\bar{K})}{(i\bar{\omega} - \mathbf{v}_{F,\sigma} \cdot \bar{\mathbf{k}})^2} \times [G_\sigma(K) - G_\sigma(K + \bar{K})]. \quad (4.9)$$

If we had simply set the vertex $\Gamma^{(2,2)}$ equal to zero in Eq (4.1) and had then closed this equation by means of the Ward identity (4.5), we would have obtained a non-linear equation. Thus, the linearity of Eq. (4.9) is the result of a cancellation of non-linear terms arising from both Ward identities (4.5) and (4.7). Because the second term on the right hand side of Eq. (4.9) is a convolution, we can easily solve this equation by means of a Fourier transformation to imaginary time and real space. Defining

$$G_\sigma(X) = \int_K e^{i(\mathbf{k} \cdot \mathbf{r} - \omega\tau)} G_\sigma(K), \quad (4.10)$$

$$H_{\Lambda,\sigma}(X) = \int_{\bar{K}} e^{i(\bar{\mathbf{k}} \cdot \mathbf{r} - \bar{\omega}\tau)} \frac{\dot{F}_{\sigma\sigma}(\bar{K})}{(i\bar{\omega} - \mathbf{v}_{F,\sigma} \cdot \bar{\mathbf{k}})^2}, \quad (4.11)$$

where $X = (\mathbf{r}, \tau)$, the flow equation (4.9) is transformed to

$$[\partial_\Lambda - H_{\Lambda,\sigma}(X) + H_{\Lambda,\sigma}(0)] G_\sigma(X) = 0. \quad (4.12)$$

This implies the conservation law

$$\partial_\Lambda \left[\exp \left\{ \int_0^\Lambda d\Lambda' [H_{\Lambda',\sigma}(X) - H_{\Lambda',\sigma}(0)] \right\} G_\sigma(X) \right] = 0. \quad (4.13)$$

Integrating from $\Lambda = 0$ to $\Lambda = \Lambda_0$, we obtain

$$G_\sigma(X) = G_{0,\sigma}(X) \exp [Q_\sigma(X)], \quad (4.14)$$

with

$$Q_\sigma(X) = S_\sigma(0) - S_\sigma(X), \quad (4.15)$$

and

$$\begin{aligned} S_\sigma(X) &= - \int_0^{\Lambda_0} d\Lambda' H_{\Lambda',\sigma}(X) \\ &= \int_{\bar{K}} \frac{\Theta(\Lambda_0 - |\bar{\mathbf{k}}|) F_{\sigma\sigma}(\bar{K})}{(i\bar{\omega} - \mathbf{v}_{F,\sigma} \cdot \bar{\mathbf{k}})^2} \cos(\bar{\mathbf{k}} \cdot \mathbf{r} - \bar{\omega}\tau), \end{aligned} \quad (4.16)$$

where we have used the invariance of the RPA interaction $F(\bar{K})$ under $\bar{K} \rightarrow -\bar{K}$. The solution in Eqs. (4.14)–(4.16) is well known from the functional integral approach to bosonization^{45,46,55,56} where $Q_\sigma(X)$ arises as a Debye-Waller factor from Gaussian averaging. In one dimension, Eqs. (4.14)–(4.16) can be shown⁴⁵ to be equivalent to the exact solution for the Green function of the Tomonaga-Luttinger model obtained via conventional bosonization. We have thus succeeded to calculate the single-particle Green function of the TLM entirely within the framework of the functional RG.

D. Truncation scheme based on relevance

The structure of the exact Green function of the TLM and the corresponding spectral function $A(k, \omega) = -\pi^{-1} \text{Im} G(k, \omega)$ depend crucially on the Ward identities discussed above, which in turn are only valid if the energy dispersion is strictly linear. In order to assess the validity of the linearization of the energy dispersion, it is important to develop truncations of the exact hierarchy of flow equations which do not explicitly make use of the validity of the asymptotic Ward identities. We now propose such a truncation scheme.

The coefficients generated in the expansion of a given vertex $\Gamma^{(2n,m)}(K'_1, \dots, K'_n; K_1, \dots, K_n; \bar{K}_1, \dots, \bar{K}_m)$ in powers of frequencies and momenta have decreasing scaling dimensions, so that the most relevant part of any vertex is obtained by setting all momenta and frequencies equal to zero. This classification leads to a simple truncation scheme: We retain only those vertices whose leading (momentum- and frequency-independent) part has a positive or vanishing scaling dimension, corresponding to relevant or marginal couplings in the usual RG jargon. In the context of calculating the critical temperature of the weakly interacting Bose gas in three dimensions, such a truncation procedure has recently been shown to give very accurate results.⁵⁷

To begin with, let us classify all couplings according to their relevance. With the rescaling defined in Sec. III D, for $D = z_\psi = z_\varphi = 1$, the scaling dimensions of the vertices $\tilde{\Gamma}^{(2n,m)}$ are $D^{(2n,m)} = 2 - n - m$, see Eq. (3.34). Hence the vertex $\tilde{\Gamma}^{(2,2)}$ as well as the vertices $\tilde{\Gamma}^{(0,3)}$ and $\tilde{\Gamma}^{(0,4)}$, whose unrescaled versions appear on the right-hand sides of Eqs. (4.1) and (4.2), are irrelevant in the RG sense. In contrast, the momentum- and frequency-independent part of the three-legged vertex,

$$\tilde{\gamma}_l = \tilde{\Gamma}^{(2,1)}(0; 0; 0) = \left(\frac{\Lambda}{\nu_0 \Omega_\Lambda} \right)^{1/2} Z_l \Gamma^{(2,1)}(K_0; K_0; 0), \quad (4.17)$$

is marginal.⁵⁸ Here $K_0 = (\pm k_F, \omega = 0)$. From the general flow equations (3.26) and (3.30) for the rescaled vertices we obtain the following exact flow equation for the rescaled self-energy defined in Eq. (3.24),

$$\partial_l \tilde{\Sigma}_l(Q) = \left(1 - \eta_l + Q \cdot \frac{\partial}{\partial Q} \right) \tilde{\Sigma}_l(Q) + \dot{\tilde{\Gamma}}_l^{(2,0)}(Q), \quad (4.18)$$

with [see Eq. (3.30)]

$$\dot{\tilde{\Gamma}}_l^{(2,0)}(Q) = - \frac{Z_l}{\Omega_\Lambda} \Lambda \partial_\Lambda \Gamma_\Lambda^{(2,0)}(K). \quad (4.19)$$

We restrict ourselves to spin-less fermions here and choose $\Omega_\Lambda = \bar{\Omega}_\Lambda = v_F \Lambda$, so that with $\nu_0 = (\pi v_F)^{-1}$ the prefactor in Eq. (4.17) turns out to be $(\frac{\Lambda}{\nu_0 \Omega_\Lambda})^{1/2} = \pi^{1/2}$. As usual, the fermionic wave-function renormalization factor Z_l is defined via

$$Z_l = \left[1 - \frac{\partial \Sigma(K)}{\partial(i\omega)} \Big|_{K=0} \right]^{-1} = 1 + \frac{\partial \tilde{\Sigma}_l(Q)}{\partial(i\epsilon)} \Big|_{Q=0}, \quad (4.20)$$

so that the flowing anomalous dimension of the fermion fields defined in Eq. (3.25) is given by

$$\eta_l = - \frac{\partial \dot{\tilde{\Gamma}}_l^{(2,0)}(Q)}{\partial(i\epsilon)} \Big|_{Q=0}. \quad (4.21)$$

According to Eq. (4.18) the constant part of the self-energy,

$$\tilde{r}_l = \tilde{\Sigma}_l(0), \quad (4.22)$$

is relevant and satisfies

$$\partial_l \tilde{r}_l = (1 - \eta_l) \tilde{r}_l + \dot{\tilde{\Gamma}}_l^{(2,0)}(0). \quad (4.23)$$

In general, \tilde{r}_l will only flow into the fixed point if the initial coupling \tilde{r}_0 is properly fine-tuned. Apart from Z_l , there are two more marginal couplings. The first is the Fermi velocity renormalization factor²⁰

$$\tilde{v}_l = Z_l + \frac{\partial \tilde{\Sigma}_l(Q)}{\partial q} \Big|_{Q=0}, \quad (4.24)$$

and the second marginal coupling is the momentum- and frequency-independent part $\tilde{\gamma}_l$ of the rescaled three-legged vertex given in Eq. (4.17). The exact flow equations for \tilde{v}_l and $\tilde{\gamma}_l$ are

$$\partial_l \tilde{v}_l = -\eta_l \tilde{v}_l + \frac{\partial \dot{\tilde{\Gamma}}_l^{(2,0)}(Q)}{\partial q} \Big|_{Q=0}, \quad (4.25)$$

and

$$\partial_l \tilde{\gamma}_l = -\eta_l \tilde{\gamma}_l + \dot{\tilde{\Gamma}}_l^{(2,1)}(0; 0; 0). \quad (4.26)$$

Note that if we retain only relevant and marginal couplings, then in the momentum transfer cutoff scheme the rescaled fermionic Green function defined in Eq. (3.32) is in $D = 1$ simply approximated by

$$\tilde{G}(Q) \approx \frac{1}{i\epsilon - \tilde{v}_l q - \tilde{r}_l}. \quad (4.27)$$

In order to make progress, we have to approximate the inhomogeneities $\dot{\tilde{\Gamma}}_l^{(2,0)}(Q)$ and $\dot{\tilde{\Gamma}}_l^{(2,1)}(0; 0; 0)$. In Sec. III E we have proposed an approximation scheme which retains only the skeleton elements of the two-point functions. In the momentum transfer cutoff scheme, the corresponding flow equations (3.35, 3.36, 3.37) further simplify because we should omit all terms involving the fermionic single scale propagator. Unfortunately, the resulting non-linear integro-differential equations still cannot be solved analytically. In order to simplify these equations further, let us replace the three-legged vertex on the right-hand sides of these equations by its marginal part. In this approximation we obtain from Eq. (3.35)

$$\dot{\tilde{\Gamma}}_l^{(2,0)}(Q) \approx \tilde{\gamma}_l^2 \int_{\bar{Q}} \dot{\tilde{F}}(\bar{Q}) \tilde{G}(Q + \bar{Q}), \quad (4.28)$$

and from Eq. (3.37)

$$\dot{\tilde{\Gamma}}_l^{(2,1)}(0; 0; 0) \approx \tilde{\gamma}_l^3 \int_{\bar{Q}} \dot{\tilde{F}}(\bar{Q}) \tilde{G}^2(\bar{Q}). \quad (4.29)$$

In order to be consistent, we should approximate $\tilde{G}(Q)$ in Eqs. (4.28) and (4.29) by Eq. (4.27). Then it is easy to see that the second term on the right-hand sides of the flow equations (4.25) and (4.26) exactly cancels the contribution from the anomalous dimension, so that

$$\partial_l \tilde{\gamma}_l = 0, \quad \partial_l \tilde{v}_l = 0. \quad (4.30)$$

For explicit calculations, let us assume that the usual couplings of the TLM are $g_2 = g_4 = f_0$, so that

$$\dot{\tilde{F}}(\bar{Q}) = \delta(1 - |\bar{q}|) \frac{\tilde{f}_0(\bar{q}^2 + \epsilon^2)}{(1 + \tilde{f}_0)\bar{q}^2 + \epsilon^2}, \quad (4.31)$$

where $\tilde{f}_0 = \nu_0 f_0$. From Eqs. (4.21) and (4.28) we then find that the anomalous dimension $\eta = \eta_l$ does not flow and is given by^{59,60}

$$\eta = \frac{\tilde{f}_0^2}{2\sqrt{1 + \tilde{f}_0} \left[\sqrt{1 + \tilde{f}_0} + 1 \right]^2}, \quad (4.32)$$

which agrees exactly with the bosonization result.⁴⁵ We emphasize that Eq. (4.32) is the correct anomalous dimension of the TLM even for $\tilde{f}_0 \gg 1$, so that, at least as far as the calculation of η is concerned, the validity of our simple truncation is not restricted to the weak coupling regime. Recall that the restriction to weak coupling is one of the shortcomings of the conventional fermionic functional RG,^{14,15,16,17,19,20,21,22,23,24,25,26} which was implemented for the TLM in Ref. 20. Because η is finite, the bare vertex $\Gamma^{(2,1)}(K_0; K_0; 0)$ actually diverges for $\Lambda \rightarrow 0$. However, the renormalized vertex $\tilde{\gamma}_l \propto Z_l \Gamma^{(2,1)}(K_0; K_0; 0)$ remains finite due to the vanishing wave-function renormalization

$$Z = e^{-\eta l} = \left(\frac{\Lambda}{\Lambda_0} \right)^\eta. \quad (4.33)$$

Integrating the flow equation (4.18) for the self-energy with the inhomogeneity approximated by Eqs. (4.28) and (4.27), we obtain, after going back to physical variables⁵⁹

$$\Sigma(k_F + k, i\omega) = - \int_{-\Lambda_0}^{\Lambda_0} \frac{d\bar{k}}{2\pi} \int_{-\infty}^{\infty} \frac{d\bar{\omega}}{2\pi} f^{\text{RPA}}(\bar{k}, i\bar{\omega}) \left(\frac{\Lambda_0}{|\bar{k}|} \right)^\eta \times \frac{1}{i(\omega + \bar{\omega}) - v_F(k + \bar{k})}, \quad (4.34)$$

where the RPA screened interaction is

$$f^{\text{RPA}}(\bar{k}, i\bar{\omega}) = f_0 \frac{v_F^2 \bar{k}^2 + \bar{\omega}^2}{v_c^2 \bar{k}^2 + \bar{\omega}^2}. \quad (4.35)$$

Here $v_c = v_F \sqrt{1 + \tilde{f}_0}$ is the velocity of collective charge excitations. Eq. (4.34) resembles the GW approximation,⁵⁴ but with the RPA interaction multiplied by an additional singular vertex correction $(\Lambda_0/|\bar{k}|)^\eta$. The explicit evaluation of Eq. (4.34) is rather tedious and will not be further discussed in this work. The resulting spectral function $A(k, \omega)$ agrees at $k = k_F$ with the bosonization result (even at strong coupling), but has the wrong threshold singularities for $|\omega| \rightarrow v_c|(k \pm k_F)|$. So far we have not been able to find a reasonably simple truncation of the exact flow equations which completely produces the spectral line shape of $A(k, \omega)$, as predicted by bosonization. Whether a self-consistent numerical solution of the truncation discussed in Sec. III E [see Eqs. (3.35)-(3.37)] would reproduce the correct spectral line-shape or not remains an open problem. The numerical solution of these equations seems to be rather difficult and is beyond the scope of this work.

V. SUMMARY AND OUTLOOK

In this work we have developed a new formulation of the functional RG for interacting fermions, which is based on the explicit introduction of collective bosonic degrees of freedom via a suitable Hubbard-Stratonovich transformation. A similar strategy has been used previously in

Refs. 36, 37, and 38. However, on the technical level the practical implementation of this method presented here differs considerable from previous works. We have payed particular attention to asymptotic Ward identities, which play a crucial role if the interaction is dominated by small momentum transfer. In one dimension, this is the key to obtain the exact solution of the Tomonaga-Luttinger model entirely within the functional RG. By using the momentum transfer associated with the bosonic field as a cutoff parameter, we have formulated the functional RG in such a way that the RG flow does not violate the Ward identities. In fact, we have shown that Ward identities emerge as the solution of the infinite hierarchy of coupled RG flow equations for the one-line irreducible vertices involving two external fermion legs and an arbitrary number of boson legs.

In this work we have mainly laid the theoretical foundation of our approach and developed an efficient method to keep track of all terms. In future work, we are planning to apply our technique to physically interesting problems. Let us mention here some problems where it might be advantageous to use our approach:

(a) *Strong coupling fixed points.* One of the big drawbacks of the conventional (purely fermionic) functional RG used by many authors^{14,15,16,17,22,23,24,25,26} is that in practice the frequency dependence of the four-point vertex $\Gamma^{(4)}$ has to be neglected, so that the wave-function renormalization factor is $Z = 1$. Although the resulting runaway flow of the vertices to strong coupling at a finite scale can be interpreted in terms of corresponding instabilities, there is the possibility that for small Z the renormalized effective interaction $Z^2\Gamma^{(4)}$ remains finite even though the bare vertex $\Gamma^{(4)}$ seems to diverge.²⁹ In our approach, the effective interaction acquires a frequency-dependence even within the lowest-order approximation. In fact, if we ignore vertex corrections, the effective interaction is simply given by the RPA. Hence, strong coupling fixed points might be accessible within our approach. Recall that the rather simple truncation of Sec. IV D gave the exact anomalous dimension of the TLM for arbitrary strength of the interaction. Possibly, more elaborate truncations of the exact hierarchy of RG flow equations (for example, the truncation based on retaining skeleton elements of the two-point functions discussed in Sec. III E, see Fig. 9) will give accurate results for the spectral properties.

(b) *Non-universal effects in one-dimensional metals.* If we do not linearize the energy dispersion in one dimension, there should be a finite momentum scale k_c (depending on the interaction and the band curvature) below which typical scaling behavior predicted by the TLM emerges. The calculation of k_c as well as the associated non-universal spectral line-shape are difficult within bosonization.⁶¹ On the other hand, within the framework of the functional RG the inclusion of irrelevant couplings is certainly possible, so that with our method it might be possible to shed some new light onto this old problem. For an explicit calculation of an entire crossover scal-

ing function between the critical regime and the short-wavelength regime of interacting bosons in $D = 3$ see Ref. 57. An analogous calculation of the dynamic scaling functions for interacting fermions in one dimension remains to be done.

(c) *Itinerant ferromagnetism.* Spontaneous ferromagnetism in Fermi systems is driven by sufficiently strong interactions involving small momentum transfers. Assuming a given form of the ferromagnetic susceptibility, Altshuler, Ioffe, and Millis⁶² concluded on the basis of an elaborate diagrammatic analysis that in the vicinity of the paramagnetic-ferromagnetic quantum-critical point in dimensions $D = 2$ a simple one-loop calculation already yields the correct qualitative behavior of the electronic self-energy. If this is correct, then in this problem vertex corrections are irrelevant. Unfortunately, due to the peculiar momentum and frequency dependence of the ferromagnetic susceptibility $\chi(\mathbf{k}, \bar{\omega})$ at the critical point, the assumption of asymptotic velocity conservation [see Eq. (C13) in Appendix C] leading to the Ward identity (4.5)-(4.7) is not justified. Note, however, that in Ref. 62 the form of the susceptibility is assumed to be given. The feedback of the collective ferromagnetic fluctuations on the non-Fermi-liquid form of the electronic properties has not been discussed. The fact that in $D < 3$ the leading interaction corrections to the inverse susceptibility $\chi^{-1}(\bar{\mathbf{k}}, \bar{\omega})$ generate a non-analytic momentum dependence^{63,64} suggests that the problem should be reconsidered taking the interplay between fermionic single-particle excitations and collective magnetic fluctuations into account. The formalism developed in this work might be suitable to shed some new light also onto this problem. The electronic properties of a two-dimensional Fermi system in the vicinity of a ferromagnetic instability have recently been studied in Ref. 65. However, these authors focused on the finite-temperature properties of the phase transition; they did not attempt to calculate the fermionic single-particle Green function in the vicinity of the zero-temperature phase transition. Note also that for sufficiently strong interactions even one-dimensional fermions can in principle have a ferromagnetic instability if the energy dispersion is non-linear.^{66,67}

(d) *Quantum phase transitions and symmetry breaking.* Our method unifies the traditional approach to quantum-phase transitions pioneered by Hertz⁹ with the modern developments in the field of fermionic functional RG, so that it might simplify the theoretical description of quantum phase transitions in situations where the fermions cannot be completely integrated out. Note that in order to describe quantum phase transitions in interacting Fermi systems within the framework of the traditional Ginzburg-Landau approach, all soft modes in the system should be explicitly retained.¹¹ In the purely fermionic functional RG^{14,15,16,17,18,19,20,21,22,23,24,25,26} symmetry breaking manifests itself via the divergence of the relevant order-parameter susceptibility; the symmetry broken phase is difficult to describe within this approach. On the other hand, in our approach the order param-

ter can be introduced explicitly as a bosonic field, which acquires a vacuum expectation value in the symmetry broken phase. Previously, a similar approach has been developed in Ref. 38 to study antiferromagnetism in the two-dimensional Hubbard model.

In summary, we believe that the formulation of the exact functional RG presented in this work will be quite useful in many different physical contexts.

ACKNOWLEDGMENTS

This work was completed while two of us (F.S. and P. K.) participated at the *Winter School on Renormalization Group Methods for Interacting Electrons* at *The International Center of Condensed Matter Physics (IC-CMP)* of the University of Brasília, Brazil. This gave us the opportunity to discuss the subtleties of the functional RG for Fermi systems with many colleagues – we thank all of them. We also thank Alvaro Ferraz and the very friendly staff of the ICCMP for their hospitality. This work was financially supported by the DFG, grant No. KO 1442/5-3 (F.S. and P.K.) and grant No. BA 2263/1-1 (L.B.).

APPENDIX A: TREE EXPANSION OF CONNECTED GREEN FUNCTIONS IN TERMS OF ONE-LINE IRREDUCIBLE VERTICES

In this Appendix we show explicitly that the vertices $\Gamma_{\alpha_1 \dots \alpha_n}^{(n)}$ defined in terms of the functional Taylor expansion of $\Gamma[\Phi]$ in Eq. (2.44) are indeed one-line irreducible. This is usually¹⁰ done graphically by taking higher order derivatives of the relation (2.40) between the second functional derivatives of $\mathcal{L}[\Phi]$ and $\mathcal{G}_c[J]$. With the help of our compact notation we can even give the tree expansion of the connected Green function in terms of one-line irreducible vertices in closed form. To do so, it is advantageous to define the functional

$$\mathbf{U} = \left[\frac{\delta^{(2)}\Gamma}{\delta\Phi\delta\Phi} - \frac{\delta^{(2)}\Gamma}{\delta\Phi\delta\Phi} \Big|_{\Phi=0} \right]^T = \left[\frac{\delta^{(2)}\Gamma}{\delta\Phi\delta\Phi} \right]^T - \boldsymbol{\Sigma}, \quad (\text{A1})$$

which is a matrix in super-index space. With this definition, we have

$$\frac{\delta^{(2)}\mathcal{L}}{\delta\Phi\delta\Phi} = \mathbf{U}^T - [\mathbf{G}^{-1}]^T, \quad (\text{A2})$$

so that

$$\begin{aligned} \left[\frac{\delta^{(2)}\mathcal{L}}{\delta\Phi\delta\Phi} \right]^{-1} &= -\mathbf{G}^T [\mathbf{1} - \mathbf{U}^T \mathbf{G}^T]^{-1} \\ &= -\sum_{l=0}^{\infty} \mathbf{G}^T (\mathbf{U}^T \mathbf{G}^T)^l. \end{aligned} \quad (\text{A3})$$

From Eq. (2.40) we then obtain

$$\begin{aligned} \frac{\delta^{(2)}\mathcal{G}_c}{\delta J\delta J} &= \mathbf{Z} \left[\frac{\delta^{(2)}\mathcal{L}}{\delta\Phi\delta\Phi} \right]^{-1} = -\mathbf{Z}\mathbf{G}^T [\mathbf{1} - \mathbf{U}^T \mathbf{G}^T]^{-1} \\ &= -\sum_{l=0}^{\infty} \mathbf{Z}\mathbf{G}^T (\mathbf{U}^T \mathbf{G}^T)^l. \end{aligned} \quad (\text{A4})$$

We now expand both sides of Eq. (A4) in powers of the sources J and compare coefficients. For the matrix on the left-hand side we obtain from Eq. (2.22)

$$\frac{\delta^{(2)}\mathcal{G}_c}{\delta J\delta J} = \sum_{n=0}^{\infty} \frac{1}{n!} \int_{\alpha_1} \dots \int_{\alpha_n} \left[\mathbf{G}_{c,\alpha_1 \dots \alpha_n}^{(n+2)} \right]^T J_{\alpha_1} \dots J_{\alpha_n}, \quad (\text{A5})$$

where the matrix $\mathbf{G}_{c,\alpha_1 \dots \alpha_n}^{(n+2)}$ is defined by

$$[\mathbf{G}_{c,\alpha_1 \dots \alpha_n}^{(n+2)}]_{\alpha\alpha'} = \mathcal{G}_{c,\alpha\alpha'\alpha_1 \dots \alpha_n}^{(n+2)}. \quad (\text{A6})$$

On the right-hand side we use Eqs. (A1) and (2.44) to write

$$\mathbf{U} = \sum_{n=1}^{\infty} \frac{1}{n!} \int_{\alpha_1} \dots \int_{\alpha_n} \boldsymbol{\Gamma}_{\alpha_1, \dots, \alpha_n}^{(n+2)} \Phi_{\alpha_1} \dots \Phi_{\alpha_n}, \quad (\text{A7})$$

where

$$[\boldsymbol{\Gamma}_{\alpha_1, \dots, \alpha_n}^{(n+2)}]_{\alpha\alpha'} = \Gamma_{\alpha\alpha'\alpha_1 \dots \alpha_n}^{(n+2)}. \quad (\text{A8})$$

To compare terms with the same powers of the sources J on both sides of Eq. (A4), we need to express the fields Φ_α on the right-hand side of Eq. (A7) in terms of the sources, using Eqs. (2.22) and (2.35),

$$\Phi_\alpha = \frac{\delta\mathcal{G}_c}{\delta J_\alpha} = \sum_{m=0}^{\infty} \frac{1}{m!} \int_{\beta_1} \dots \int_{\beta_m} \mathcal{G}_{c,\alpha\beta_1 \dots \beta_m}^{(m+1)} J_{\beta_1} \dots J_{\beta_m}. \quad (\text{A9})$$

Substituting Eqs. (A5), (A7) and (A9) into Eq. (A4) and comparing terms with the same powers of the sources (after symmetrization), we obtain a general relation between the connected and the one-line irreducible correlation functions

$$\begin{aligned} \mathbf{G}_{c,\beta_1, \dots, \beta_n}^{(n+2)} &= -\sum_{l=0}^{\infty} \sum_{n_1, \dots, n_l=1}^{\infty} \frac{1}{n_1! \dots n_l!} \\ &\quad \times \int_{\alpha_1^1} \dots \int_{\alpha_{n_1}^1} \dots \int_{\alpha_1^l} \dots \int_{\alpha_{n_l}^l} \\ &\quad \times \sum_{m_1^1, \dots, m_{n_1}^1=1}^{\infty} \dots \sum_{m_1^l, \dots, m_{n_l}^l=1}^{\infty} \delta_{n, \sum_{i=1}^l \sum_{j=1}^{n_i} m_j^i} \\ &\quad \times \left[\mathbf{Z}\mathbf{G}^T \boldsymbol{\Gamma}_{\alpha_1^1, \dots, \alpha_{n_1}^1}^{(n_1+2)T} \mathbf{G}^T \dots \mathbf{G}^T \boldsymbol{\Gamma}_{\alpha_1^l, \dots, \alpha_{n_l}^l}^{(n_l+2)T} \mathbf{G}^T \right]^T \\ &\quad \times \mathcal{S}_{\beta_1, \dots, \beta_{m_1^1}; \dots; \beta_{n-n_l}^{l+1}, \dots, \beta_n} \left\{ \mathcal{G}_{c,\alpha_1^1, \beta_1, \dots, \beta_{m_1^1}}^{(m_1^1+1)} \right. \\ &\quad \left. \dots \mathcal{G}_{c,\alpha_{n_l}^l, \beta_{n-n_l+1}, \dots, \beta_n}^{(m_{n_l}^l+1)} \right\}. \end{aligned} \quad (\text{A10})$$

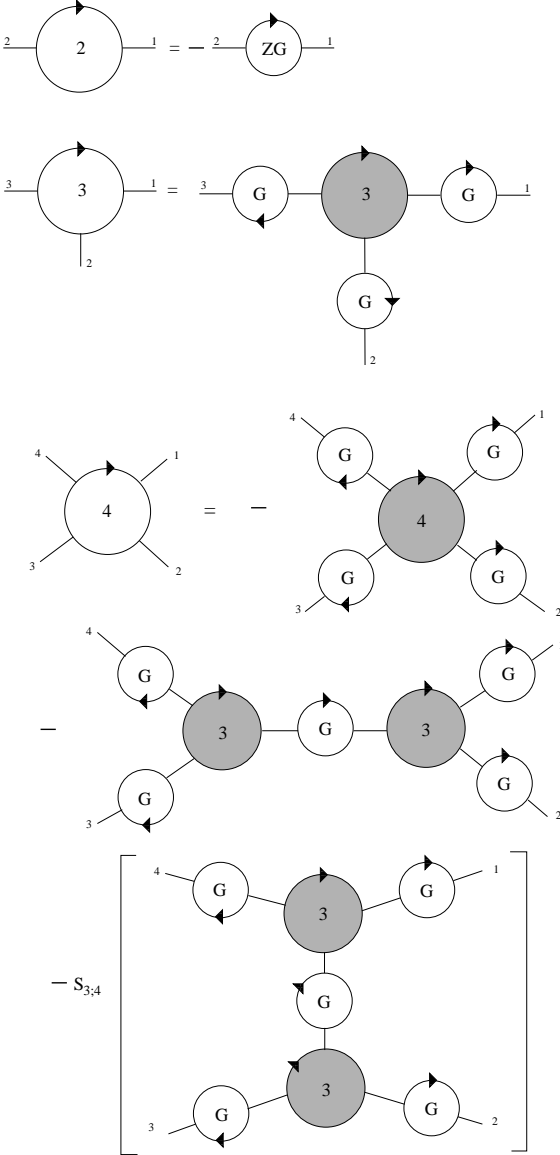


FIG. 15: Graphical representation of the relation between connected Green functions and one-line irreducible vertices up to the four-point functions. The irreducible vertices are represented by shaded oriented circles with the appropriate number of legs, see Fig. 1. The connected Green functions are drawn as empty oriented circles with a number indicating the number of external legs.

On the right-hand side of this rather cumbersome expression, only connected correlation functions with degree smaller than on the left-hand side appear. One can therefore recursively express all connected correlation functions via their one-line irreducible counterparts. Only a finite number of terms contribute on the right-hand side. The operator \mathcal{S} symmetrizes the expression in curly brackets with respect to indices on different correlation functions, i.e., it generates all permutations of the indices with appropriate signs, counting expressions

only once that are generated by permutations of indices on the same vertex. More precisely the action of \mathcal{S} is given by ($m = \sum_{i=1}^l m_i$)

$$\mathcal{S}_{\alpha_1, \dots, \alpha_{m_1}; \dots; \alpha_{m-m_l+1}, \dots, \alpha_m} \{A_{\alpha_1, \dots, \alpha_m}\} = \frac{1}{\prod_i m_i!} \sum_P \text{sgn}_\zeta(P) A_{\alpha_{P(1)}, \dots, \alpha_{P(m)}}, \quad (\text{A11})$$

where P denotes a permutation of $\{1, \dots, m\}$ and sgn_ζ is the sign created by permuting field variables according to the permutation P , i.e.,

$$\Phi_{\alpha_1} \cdot \dots \cdot \Phi_{\alpha_m} = \text{sgn}_\zeta(P) \Phi_{\alpha_{P(1)}} \cdot \dots \cdot \Phi_{\alpha_{P(m)}}. \quad (\text{A12})$$

A diagrammatic representation of the first few terms of the tree-expansion generated by Eq. (A10) is given in Fig. 15. Let us give the corresponding analytic expressions: If we set $n = 0$ in Eq. (A10) then only the term with $l = 0$ contributes and we obtain

$$\mathbf{G}_c^{(2)} = -\mathbf{ZG} = -\mathbf{G}^T, \quad (\text{A13})$$

which is Eq. (2.24) in matrix form. For $n = 1$ the single term with $l = 1$, $n_1 = 1$, $m_1^1 = 1$ contributes on the right-hand side of Eq. (A10). Using $\mathbf{ZG} = \mathbf{G}^T$ the tree expansion of the connected Green function with three external legs can be written as

$$\mathcal{G}_{c, \beta_1 \beta_2 \beta_3}^{(3)} = \int_{\alpha_1} \int_{\alpha_2} \int_{\alpha_3} [\mathbf{G}]_{\beta_1 \alpha_1} [\mathbf{G}]_{\beta_2 \alpha_2} [\mathbf{G}]_{\beta_3 \alpha_3} \Gamma_{\alpha_1 \alpha_2 \alpha_3}^{(3)}. \quad (\text{A14})$$

Finally, consider the connected Green function with four external legs, corresponding to $n = 2$ in Eq. (A10). In this case the following three terms contribute,

| term | l | n_i | m_j^i |
|------|-----|-----------------|---------------------|
| 1.) | 1 | $n_1 = 1$ | $m_1^1 = 2$ |
| 2.) | 1 | $n_1 = 2$ | $m_1^1 = m_2^1 = 1$ |
| 3.) | 2 | $n_1 = n_2 = 1$ | $m_1^1 = m_1^2 = 1$ |

The corresponding analytic expression is

$$\begin{aligned} \mathcal{G}_{c, \beta_1 \beta_2 \beta_3 \beta_4}^{(4)} &= \\ &- \int_{\alpha_1} \dots \int_{\alpha_4} [\mathbf{G}]_{\beta_1 \alpha_1} [\mathbf{G}]_{\beta_2 \alpha_2} [\mathbf{G}]_{\beta_3 \alpha_3} [\mathbf{G}]_{\beta_4 \alpha_4} \Gamma_{\alpha_1 \alpha_2 \alpha_3 \alpha_4}^{(4)} \\ &- \int_{\alpha_1} \dots \int_{\alpha_6} [\mathbf{G}]_{\beta_1 \alpha_1} [\mathbf{G}]_{\beta_2 \alpha_2} [\mathbf{G}]_{\beta_3 \alpha_3} [\mathbf{G}]_{\beta_4 \alpha_4} \\ &\quad \times \Gamma_{\alpha_1 \alpha_2 \alpha_5}^{(3)} [\mathbf{G}]_{\alpha_5 \alpha_6} \Gamma_{\alpha_6 \alpha_3 \alpha_4}^{(3)} \\ &- \int_{\alpha_1} \dots \int_{\alpha_6} S_{\beta_3; \beta_4} \left\{ [\mathbf{G}]_{\beta_1 \alpha_1} [\mathbf{G}]_{\beta_2 \alpha_2} [\mathbf{G}]_{\beta_3 \alpha_3} [\mathbf{G}]_{\beta_4 \alpha_4} \right. \\ &\quad \left. \times \Gamma_{\alpha_1 \alpha_5 \alpha_4}^{(3)} [\mathbf{G}]_{\alpha_5 \alpha_6} \Gamma_{\alpha_6 \alpha_2 \alpha_3}^{(3)} \right\}. \end{aligned} \quad (\text{A15})$$

APPENDIX B: DYSON-SCHWINGER EQUATIONS AND SKELETON DIAGRAMS

In this appendix we show how the skeleton diagrams for the two-point functions and the three-legged vertex in

Fig. 8 can be formally derived from the Dyson-Schwinger equations of motion. Although the skeleton graphs are usually written down directly from topological considerations of the structure of diagrammatic perturbation theory,³³ it is instructive to see how the skeleton expansion of the irreducible vertices can be derived formally within our functional integral approach.

The invariance of the generating functional $\mathcal{G}[J]$ of the Green functions defined in Eq. (2.18) with respect to infinitesimal shifts in the integration variables Φ_α implies the Dyson-Schwinger equations of motion⁶⁸

$$\left(\zeta_\alpha J_\alpha - \frac{\delta S}{\delta \Phi_\alpha} \left[\frac{\delta}{\delta J_\alpha} \right] \right) \mathcal{G}[J_\alpha] = 0. \quad (\text{B1})$$

For our coupled Fermi-Bose system with Euclidean action $S[\bar{\psi}, \psi, \varphi]$ given by Eqs. (2.2, 2.6, 2.7, 2.8) involving three types of fields Eq. (B1) is actually equivalent with the following three equations,

$$\begin{aligned} & \left(J_{-\bar{K}\sigma} - \sum_{\sigma'} [f_{\bar{\mathbf{k}}}^{-1}]^{\sigma'\sigma} \frac{\delta}{\delta J_{\bar{K}\sigma'}} \right) \mathcal{G} \\ & - i\zeta \int_K \frac{\delta^{(2)}\mathcal{G}}{\delta j_{K+\bar{K}\sigma} \delta \bar{J}_{K\sigma}} = 0, \end{aligned} \quad (\text{B2})$$

$$\begin{aligned} & \left(\zeta \bar{J}_{K\sigma} + [i\omega - \xi_{\mathbf{k}\sigma}] \frac{\delta}{\delta j_{K\sigma}} \right) \mathcal{G} \\ & - i \int_{\bar{K}} \frac{\delta^{(2)}\mathcal{G}}{\delta j_{K+\bar{K}\sigma} \delta J_{-\bar{K}\sigma}} = 0, \end{aligned} \quad (\text{B3})$$

$$\begin{aligned} & \left(j_{K\sigma} + [i\omega - \xi_{\mathbf{k}\sigma}] \frac{\delta}{\delta \bar{J}_{K\sigma}} \right) \mathcal{G} \\ & - i \int_{\bar{K}} \frac{\delta^{(2)}\mathcal{G}}{\delta \bar{J}_{K-\bar{K}\sigma} \delta J_{-\bar{K}\sigma}} = 0. \end{aligned} \quad (\text{B4})$$

Expressing these equations in terms of the generating functionals $\mathcal{G}_c[\bar{j}, j, J]$ of the connected Green functions and the corresponding generating functional $\Gamma[\bar{\psi}, \psi, \varphi]$ of the irreducible vertices defined in Eq. (2.42), we obtain the Dyson-Schwinger equations of motion in the following form,

$$\frac{\delta \Gamma}{\delta \varphi_{\bar{K}\sigma}} - i \int_K \left[\bar{\psi}_{K+\bar{K},\sigma} \psi_{K\sigma} + \frac{\delta^{(2)}\mathcal{G}_c}{\delta \bar{J}_{K\sigma} \delta j_{K+\bar{K},\sigma}} \right] = 0, \quad (\text{B5})$$

$$\frac{\delta \Gamma}{\delta \psi_{K\sigma}} - i \int_{\bar{K}} \left[\zeta \bar{\psi}_{K+\bar{K},\sigma} \varphi_{\bar{K}\sigma} + \frac{\delta^{(2)}\mathcal{G}_c}{\delta j_{K+\bar{K},\sigma} \delta J_{-\bar{K}\sigma}} \right] = 0, \quad (\text{B6})$$

$$\frac{\delta \Gamma}{\delta \bar{\psi}_{K\sigma}} - i \int_{\bar{K}} \left[\psi_{K-\bar{K},\sigma} \varphi_{\bar{K}\sigma} + \frac{\delta^{(2)}\mathcal{G}_c}{\delta \bar{J}_{K-\bar{K},\sigma} \delta J_{-\bar{K}\sigma}} \right] = 0. \quad (\text{B7})$$

The second functional derivatives of \mathcal{G}_c can be expressed in terms of the irreducible vertices using Eq. (A4). Taking derivatives of Eqs. (B5–B7) with respect to the fields

and then setting the fields equal to zero we obtain the desired skeleton expansions of the irreducible vertices. Let us start with the skeleton diagram for the self-energy shown in Fig. 8 (a). To derive this, we simply differentiate Eq. (B7) with respect to $\psi_{K'\sigma}$. Using

$$\frac{\delta^{(2)}\Gamma}{\delta \psi_{K'\sigma} \delta \bar{\psi}_{K\sigma}} \Big|_{\text{fields}=0} = \delta_{K,K'} \Sigma_\sigma(K), \quad (\text{B8})$$

we obtain

$$\delta_{K,K'} \Sigma_\sigma(K) = i \int_{\bar{K}} \frac{\delta^{(3)}\mathcal{G}_c}{\delta \psi_{K'\sigma} \delta \bar{J}_{K-\bar{K},\sigma} \delta J_{-\bar{K}\sigma}} \Big|_{\text{fields}=0}. \quad (\text{B9})$$

From the $l=1$ term in the expansion (A4) it is easy to show that

$$\begin{aligned} & \frac{\delta^{(3)}\mathcal{G}_c}{\delta \psi_{K'\sigma} \delta \bar{J}_{K-\bar{K},\sigma} \delta J_{-\bar{K}\sigma}} \Big|_{\text{fields}=0} = \delta_{K,K'} F_{\sigma\sigma}(\bar{K}) \\ & \times G_\sigma(K + \bar{K}) \Gamma^{(2,1)}(K + \bar{K}\sigma; K\sigma; \bar{K}\sigma), \end{aligned} \quad (\text{B10})$$

so that

$$\Sigma_\sigma(K) = i \int_{\bar{K}} F_{\sigma\sigma}(\bar{K}) G_\sigma(K + \bar{K}) \Gamma^{(2,1)}(K + \bar{K}\sigma; K\sigma; \bar{K}\sigma), \quad (\text{B11})$$

which is the analytic expression for the skeleton graph shown in Fig. 8 (a). Similarly, we obtain the skeleton expansion of the irreducible polarization by differentiating Eq. (B5) with respect to $\varphi_{-\bar{K}\sigma}$,

$$\begin{aligned} \Pi_\sigma(\bar{K}) &= i \int_K \frac{\delta^{(3)}\mathcal{G}_c}{\delta \varphi_{-\bar{K}\sigma} \delta \bar{J}_{K,\sigma} \delta j_{K+\bar{K}\sigma}} \Big|_{\text{fields}=0} \\ &= -i\zeta \int_K G_\sigma(K) G_\sigma(K + \bar{K}) \Gamma^{(2,1)}(K + \bar{K}\sigma; K\sigma; \bar{K}\sigma), \end{aligned} \quad (\text{B12})$$

which is shown diagrammatically in Fig. 8 (b). Finally, applying the operator $\frac{\delta^{(2)}\Gamma}{\delta \psi_{K+\bar{K}\sigma} \delta \psi_{K\sigma}}$ to Eq. (B5) and subsequently setting the fields equal to zero we obtain the skeleton expansion of the three-legged vertex shown in Fig. 8 (c),

$$\begin{aligned} \Gamma^{(2,1)}(K + \bar{K}\sigma; K\sigma; \bar{K}\sigma) &= i \\ & -i\zeta \int_{K'} G_\sigma(K') G_\sigma(K' + \bar{K}) \\ & \times \Gamma^{(4,0)}(K + \bar{K}\sigma, K'\sigma; K' + \bar{K}\sigma, K\sigma). \end{aligned} \quad (\text{B13})$$

Skeleton expansions for higher order vertices can be obtained analogously from the appropriate functional derivatives of Eqs. (B5–B7).

APPENDIX C: WARD IDENTITIES

In this Appendix we give a self-contained derivation of the Ward identities in Eqs. (4.5–4.7) within the framework of our functional integral approach. Although the

Ward identity (4.5) for the three-legged vertex is well known,^{42,43,44,45} it seems that the higher order Ward identities given in Eqs. (4.6) and (4.7) cannot be found anywhere in the literature. Since we are interested in deriving infinitely many Ward identities involving the vertices $\Gamma^{(2,m)}$ with two fermion legs and an arbitrary number m of boson legs, it is convenient to derive first a “master Ward identity” for the generating functional for the irreducible vertices, from which we can obtain all desired Ward identities for the vertices by taking appropriate functional derivatives.

Consider the generating functional of the Green function of our mixed Fermi-Bose theory defined in Eq. (2.18), which in explicit notation is given by

$$\mathcal{G}[\bar{j}, j, J] = \frac{1}{Z_0} \int D[\bar{\psi}, \psi, \varphi] e^{-S[\bar{\psi}, \psi, \varphi] + (\bar{j}, \psi) + (\bar{\psi}, j) + (J^*, \varphi)} . \quad (\text{C1})$$

If we rewrite the parts of the action involving the fermionic fields $\bar{\psi}$ and ψ in real space and imaginary time, the Euclidean action reads [we use again the notation $X = (\tau, \mathbf{r})$ introduced in Sec. IV C]

$$\begin{aligned} S[\bar{\psi}, \psi, \varphi] &= S_0[\bar{\psi}, \psi] + S_0[\varphi] + S_1[\bar{\psi}, \psi, \varphi] \\ S_0[\bar{\psi}, \psi] &= \sum_{\sigma} \int_X \bar{\psi}_{\sigma}(X) \partial_{\tau} \psi_{\sigma}(X) \\ &+ \sum_{\sigma} \int d\tau \int d^D r \int d^D r' \bar{\psi}_{\sigma}(\tau, \mathbf{r}) \end{aligned} \quad \times \xi_{\sigma}(\mathbf{r} - \mathbf{r}') \psi_{\sigma}(\tau, \mathbf{r}') , \quad (\text{C2})$$

$$S_1[\bar{\psi}, \psi, \varphi] = \sum_{\sigma} \int_X \bar{\psi}_{\sigma}(X) \psi_{\sigma}(X) \varphi_{\sigma}(X) , \quad (\text{C3})$$

where we have defined the Fourier transform of the dispersion

$$\xi_{\sigma}(\mathbf{r}) = \int \frac{d^D k}{(2\pi)^D} \xi_{\mathbf{k}\sigma} e^{i\mathbf{k}\cdot\mathbf{r}} . \quad (\text{C4})$$

Suppose now we perform a local gauge transformation on the fermion fields, defining new fields ψ' and $\bar{\psi}'$ via

$$\psi_{\sigma}(X) = e^{i\alpha_{\sigma}(X)} \psi'_{\sigma}(X) , \quad \bar{\psi}_{\sigma}(X) = e^{-i\alpha_{\sigma}(X)} \bar{\psi}'_{\sigma}(X) , \quad (\text{C5})$$

where $\alpha_{\sigma}(X)$ is an arbitrary real function. It is easy to show that, to linear order in $\alpha_{\sigma}(X)$, the action (C3) transforms as follows

$$\begin{aligned} S[e^{-i\alpha} \bar{\psi}', e^{i\alpha} \psi', \varphi' + \delta\varphi] &= S[\bar{\psi}', \psi', \varphi'] \\ &+ i \sum_{\sigma} \int_X \bar{\psi}'_{\sigma}(X) [\partial_{\tau} \alpha_{\sigma}(X)] \psi'_{\sigma}(X) \\ &- i \sum_{\sigma} \int d\tau \int d^D r \int d^D r' \bar{\psi}'_{\sigma}(\tau, \mathbf{r}) [\alpha_{\sigma}(\tau, \mathbf{r}) - \alpha_{\sigma}(\tau, \mathbf{r}')] \end{aligned} \quad \times \xi_{\sigma}(\mathbf{r} - \mathbf{r}') \psi'_{\sigma}(\tau, \mathbf{r}') . \quad (\text{C6})$$

Using this relation, we see that the invariance of the generating functional in Eq. (C1) with respect to the change

of integration variables defined by Eq. (C5) implies, to linear order in $\alpha_{\sigma}(X)$,

$$\begin{aligned} 0 &= \frac{1}{Z_0} \int D[\bar{\psi}, \psi, \varphi] e^{-S[\bar{\psi}, \psi, \varphi] + (\bar{j}, \psi) + (\bar{\psi}, j) + (J^*, \varphi)} \\ &\times \left\{ - \sum_{\sigma} \int_X \bar{\psi}_{\sigma}(X) [\partial_{\tau} \alpha_{\sigma}(X)] \psi_{\sigma}(X) \right. \\ &+ \sum_{\sigma} \int d\tau \int d^D r \int d^D r' \bar{\psi}_{\sigma}(\tau, \mathbf{r}) \\ &\times [\alpha_{\sigma}(\tau, \mathbf{r}) - \alpha_{\sigma}(\tau, \mathbf{r}')] \xi_{\sigma}(\mathbf{r} - \mathbf{r}') \psi_{\sigma}(\tau, \mathbf{r}') \\ &\left. + (\bar{j}, \alpha\psi) - (\bar{\psi}\alpha, j) \right\} . \quad (\text{C7}) \end{aligned}$$

Taking the functional derivative of this equation with respect to $\alpha_{\sigma}(X)$ this implies in Fourier space

$$\begin{aligned} 0 &= \int_K \left\{ [i\bar{\omega} - \xi_{\mathbf{k}+\bar{\mathbf{k}},\sigma} + \xi_{\mathbf{k}\sigma}] \frac{\delta^{(2)}\mathcal{G}}{\delta \bar{j}_{K\sigma} \delta j_{K+\bar{K}\sigma}} \right. \\ &\left. + \bar{j}_{K+\bar{K}\sigma} \frac{\delta\mathcal{G}}{\delta \bar{j}_{K\sigma}} - j_{K\sigma} \frac{\delta\mathcal{G}}{\delta j_{K+\bar{K}\sigma}} \right\} . \quad (\text{C8}) \end{aligned}$$

Expressing this equation in terms of the generating functional $\mathcal{G}_c = \ln \mathcal{G}$ of the connected Green functions and the generating functional and $\Gamma[\bar{\psi}, \psi, \varphi]$ of the irreducible vertices as defined in Eq. (2.42), we obtain

$$\begin{aligned} 0 &= \int_K \left\{ [i\bar{\omega} - \xi_{\mathbf{k}+\bar{\mathbf{k}},\sigma} + \xi_{\mathbf{k}\sigma}] \frac{\delta^{(2)}\mathcal{G}_c}{\delta \bar{j}_{K\sigma} \delta j_{K+\bar{K}\sigma}} \right. \\ &\left. + \psi_{K\sigma} \frac{\delta\Gamma}{\delta \psi_{K+\bar{K}\sigma}} - \bar{\psi}_{K+\bar{K}\sigma} \frac{\delta\Gamma}{\delta \bar{\psi}_{K\sigma}} \right\} . \quad (\text{C9}) \end{aligned}$$

Alternatively, using the Dyson-Schwinger equation (B5), we may rewrite this as

$$\begin{aligned} 0 &= i\bar{\omega} \left[\frac{\delta\Gamma}{\delta \varphi_{\bar{K}\sigma}} - i \int_K \bar{\psi}_{K+\bar{K}\sigma} \psi_{K\sigma} \right] \\ &- i \int_K (\xi_{\mathbf{k}+\bar{\mathbf{k}},\sigma} - \xi_{\mathbf{k}\sigma}) \frac{\delta^{(2)}\mathcal{G}_c}{\delta \bar{j}_{K\sigma} \delta j_{K+\bar{K}\sigma}} \\ &+ i \int_K \left[\psi_{K\sigma} \frac{\delta\Gamma}{\delta \psi_{K+\bar{K}\sigma}} - \bar{\psi}_{K+\bar{K}\sigma} \frac{\delta\Gamma}{\delta \bar{\psi}_{K\sigma}} \right] . \quad (\text{C10}) \end{aligned}$$

Eqs. (C9) and (C10) are our “master Ward identities” from which we can now obtain Ward identities for the vertices by differentiation. For example, taking the derivative $\frac{\delta}{\delta \varphi_{-\bar{K}\sigma}}$ of Eq. (C10) we obtain

$$i\bar{\omega} \Pi_{\sigma}(\bar{K}) - \Pi_{\sigma}^c(\bar{K}) = 0 , \quad (\text{C11})$$

where we have defined

$$\begin{aligned} \Pi_{\sigma}^c(\bar{K}) &= -i\zeta \int_K (\xi_{\mathbf{k}+\bar{\mathbf{k}},\sigma} - \xi_{\mathbf{k}\sigma}) G_{\sigma}(K) G_{\sigma}(K + \bar{K}) \\ &\times \Gamma^{(2,1)}(K + \bar{K}\sigma; K\sigma; \bar{K}\sigma) . \quad (\text{C12}) \end{aligned}$$

Eq. (C11) is a relation between response functions, which follows more directly from the equation of continuity. If we are interested in vertices involving at least one fermionic momentum and the momentum transferred by the interaction is small, our master Ward identities can be further simplified. Then all fermionic momenta lie close to a given point $\mathbf{k}_{F,\sigma}$ on the Fermi surface so that Eq. (C9) and (C10) become simpler if we assume asymptotic velocity conservation. This means that we replace under the integral sign

$$\xi_{\mathbf{k}+\bar{\mathbf{k}},\sigma} - \xi_{\mathbf{k}\sigma} \rightarrow \mathbf{v}_{F,\sigma} \cdot \bar{\mathbf{k}}. \quad (\text{C13})$$

This approximation amounts to the linearization of the energy dispersion relative to the point $\mathbf{k}_{F,\sigma}$ on the Fermi surface. Using again Eq. (B5), our master Ward identity becomes

$$\begin{aligned} 0 = & (i\bar{\omega} - \mathbf{v}_{F,\sigma} \cdot \bar{\mathbf{k}}) \left[\frac{\delta\Gamma}{\delta\varphi_{\bar{K}\sigma}} - i \int_K \bar{\psi}_{K+\bar{K}\sigma} \psi_{K\sigma} \right] \\ & + i \int_K \left[\psi_{K\sigma} \frac{\delta\Gamma}{\delta\psi_{K+\bar{K}\sigma}} - \bar{\psi}_{K+\bar{K}\sigma} \frac{\delta\Gamma}{\delta\bar{\psi}_{K\sigma}} \right]. \end{aligned} \quad (\text{C14})$$

Differentiating this simplified master Ward identity with

respect to the fields using the relation (B8) as well as

$$\begin{aligned} & \frac{\delta^{(3)}\Gamma}{\delta\varphi_{\bar{K}\sigma}\delta\psi_{K\sigma}\delta\bar{\psi}_{K+\bar{K}\sigma}} \Big|_{\text{fields}=0} \\ & = \Gamma^{(2,1)}(K + \bar{K}\sigma; K\sigma; \bar{K}\sigma), \end{aligned} \quad (\text{C15})$$

$$\begin{aligned} & \frac{\delta^{(4)}\Gamma}{\delta\varphi_{\bar{K}_1\sigma}\delta\varphi_{\bar{K}_2\sigma}\delta\psi_{K\sigma}\delta\bar{\psi}_{K+\bar{K}_1+\bar{K}_2\sigma}} \Big|_{\text{fields}=0} \\ & = \Gamma^{(2,2)}(K + \bar{K}_1 + \bar{K}_2\sigma; K\sigma; \bar{K}_1\sigma, \bar{K}_2\sigma), \end{aligned} \quad (\text{C16})$$

and so on, we obtain the Ward identities for the irreducible vertices given in Eqs. (4.5,4.6,4.7).

Of course, other Ward identities, e.g., the Ward identity for $\Gamma^{(4,1)}$ discussed in Ref. 47, can also be obtained from Eq. (C14). Note that if the approximation (C13) is not made, the master Ward identity (C14) should be replaced by the more general master Ward identity (C10), so that the Ward identities (4.5,4.6,4.7) for the vertices acquire correction terms. The effect of these correction terms on the Ward identities for $\Gamma^{(2,1)}$ and $\Gamma^{(4,1)}$ has recently been studied in a mathematically rigorous way by Benfatto and Mastropietro.⁴⁷

- ¹ K. G. Wilson, Phys. Rev. Lett. **28**, 548 (1972).
- ² K. G. Wilson and J. G. Kogut, Phys. Reports **12C**, 75 (1974).
- ³ For a recent review with historical remarks see M. E. Fisher, Rev. Mod. Phys. **70**, 653 (1998).
- ⁴ S. K. Ma, *Modern Theory of Critical Phenomena*, (Benjamin/Cummings, Reading, MA, 1976).
- ⁵ F. J. Wegner and A. Houghton, Phys. Rev. A **8**, 401 (1973).
- ⁶ C. Di Castro, G. Jona-Lasinio, and L. Peliti, Annals of Physics **87**, 327 (1974).
- ⁷ J. F. Nicoll, T. S. Chang, and H. E. Stanley, Phys. Lett. A **57**, 7 (1976); J. F. Nicoll and T. S. Chang, *ibid.* **62**, 287 (1977).
- ⁸ T. S. Chang, D. D. Vvedensky, and J. F. Nicoll, Phys. Rep. **217**, 279 (1992).
- ⁹ J. A. Hertz, Phys. Rev. B **14**, 1165 (1976).
- ¹⁰ J.W. Negele and H. Orland, *Quantum Many-Particle Systems*, (Addison-Wesley, Redwood City, CA 1988).
- ¹¹ T. R. Kirkpatrick and D. Belitz, Phys. Rev. B **53**, 14364 (1996); D. Belitz, T. R. Kirkpatrick, R. Narayanan, and T. Vojta, Phys. Rev. Lett. **85**, 4602 (2000); D. Belitz, T. R. Kirkpatrick, M. T. Mercaldo, and S. L. Sessions, Phys. Rev. B **63**, 174427 (2001); *ibid.* **63**, 174428 (2001); D. Belitz, T. R. Kirkpatrick, and J. Rollbühler, cond-mat/0406350.
- ¹² A. Rosch, Phys. Rev. B **64**, 174407 (2001).
- ¹³ R. Shankar, Rev. Mod. Phys. **66**, 129 (1994).
- ¹⁴ D. Zanchi and H. J. Schulz, Phys. Rev. B **54**, 9509 (1996); Europhys. Lett. **44**, 235 (1998); Phys. Rev. B **61**, 13609 (2000); Europhys. Lett. **55**, 376 (2001).
- ¹⁵ C. J. Halboth and W. Metzner, Phys. Rev. B **61**, 7364 (2000); Phys. Rev. Lett. **85**, 5162 (2000).
- ¹⁶ C. Honerkamp, M. Salmhofer, N. Furukawa, and T. M. Rice, Phys. Rev. B **63**, 35109 (2001); C. Honerkamp, Euro. Phys. J. B **21**, 81 (2001).
- ¹⁷ C. Honerkamp and M. Salmhofer, Phys. Rev. B **64**, 184516 (2001); Phys. Rev. Lett. **87**, 187004 (2001).
- ¹⁸ M. Salmhofer and C. Honerkamp, Prog. Theor. Physics **105**, 1 (2001).
- ¹⁹ P. Kopietz and T. Busche, Phys. Rev. B **64**, 155101 (2001).
- ²⁰ T. Busche, L. Bartosch, and P. Kopietz, J. Phys.: Cond. Mat. **14**, 8513 (2002).
- ²¹ S. Ledowski and P. Kopietz, J. Phys.: Condens. Matter **15**, 4779 (2003).
- ²² S. W. Tsai and B. Marston, Can. J. Phys. **79**, 1463 (2001).
- ²³ B. Binz, D. Baeriswyl and B. Douçot, Eur. Phys. J. B **25**, 69 (2002); Ann. Phys. (Leipzig) **12**, 704 (2004).
- ²⁴ V. Meden, W. Metzner, U. Schollwöck, and K. Schönhammer, Phys. Rev. B **65**, 045318 (2002).
- ²⁵ A. P. Kampf and A. A. Katanin, Phys. Rev. B **67**, 125104 (2003); A. A. Katanin and A. P. Kampf, Phys. Rev. B **68**, 195101 (2003); cond-mat/0310112; cond-mat/0408246.
- ²⁶ A. A. Katanin, cond-mat/0402602.
- ²⁷ C. Wetterich, Phys. Lett. B **301**, 90 (1993).
- ²⁸ T. R. Morris, Int. J. Mod. Phys. A **9**, 2411 (1994).
- ²⁹ A. Ferraz, Phys. Rev. B **68**, 075115 (2003); H. Freire, E. Correa, and A. Ferraz, cond-mat/0304347.
- ³⁰ A. Ferraz, Europhys. Lett. **61**, 228 (2003).
- ³¹ I. Ia. Pomeranchuk, Zh. Eksp. Teor. Fiz. **35**, 524 (1958) [Sov. Phys. JETP **8**, 361 (1958)].
- ³² W. Metzner, D. Rohe, and S. Andergassen Phys. Rev. Lett. **91**, 066402 (2003).
- ³³ P. Nozières, *Theory of Interacting Fermi Systems*, (Benjamin, New York, 1964).
- ³⁴ W. Kohn and J. M. Luttinger, Phys. Rev. **118**, 41 (1960); J. M. Luttinger, Phys. Rev. **119**, 1153 (1960).

³⁵ D. Pines and P. Nozières, *The Theory of Quantum Liquids*, Volume I, (Addison-Wesley Advanced Book Classics, Redwood City, Ca, 1989).

³⁶ S. Correia, J. Polonyi, J. Richert, cond-mat/0108048.

³⁷ C. Wetterich, cond-mat/0208361v3.

³⁸ T. Baier, E. Bick, and C. Wetterich, cond-mat/0308591 and cond-mat/0309715.

³⁹ For an up to date review see the recent book by T. Giarmarchi, *Quantum Physics in One Dimension*, (Clarendon Press, Oxford, 2004).

⁴⁰ F. D. M. Haldane, J. Phys. C: Solid State Phys. **14**, 2585 (1981).

⁴¹ M. Stone, *Bosonization*, (World Scientific, Singapore, 1994).

⁴² I. E. Dzyaloshinskii and A. I. Larkin, Zh. Eksp. Teor. Fiz. **65**, 411 (1973) [Sov. Phys. JETP **38**, 202 (1974)].

⁴³ T. Bohr, Nordita preprint 81/4, *Lectures on the Luttinger Model*, 1981 (unpublished).

⁴⁴ W. Metzner, C. Castellani, and C. Di Castro, Adv. Phys. **47**, 317 (1998).

⁴⁵ P. Kopietz, *Bosonization of Interacting Fermions in Arbitrary Dimensions*, (Springer, Berlin, 1997).

⁴⁶ P. Kopietz, J. Hermisson, and K. Schönhammer, Phys. Rev. B **52**, 10877 (1995); P. Kopietz and K. Schönhammer, Z. Phys. B **100**, 259 (1996).

⁴⁷ G. Benfatto and V. Mastropietro, cond-mat/0409049.

⁴⁸ The factor ζ arises from the antisymmetry of the Grassmann fields. Although throughout this work it is understood that $\zeta = -1$, all expressions involving the factor ζ remain valid for bosonic fields ψ and $\bar{\psi}$ if we set $\zeta = +1$. We adopt here the notation of Ref. 10.

⁴⁹ More precisely, we should distinguish the quantum field Φ_α from its expectation value, i.e., we should write $\langle \Phi_\alpha \rangle = \delta \mathcal{G}_c / \delta J_\alpha$. For notational simplicity we redefine $\langle \Phi_\alpha \rangle \rightarrow \Phi_\alpha$. Whenever we work with the Legendre effective action it is understood that Φ_α denotes the expectation value of the corresponding quantum field.

⁵⁰ J. Solyom, Adv. Phys. **28**, 201 (1979).

⁵¹ K. Schönhammer, in *Strong Interactions in Low Dimensions*, edited by D. Baeriswyl and L. Degiorgi, (Dordrecht, Kluwer, 2003); cond-mat/9710330.

⁵² C. Honerkamp, D. Rohe, S. Andergassen, and T. Enss, cond-mat/0403633.

⁵³ The factor of Ω_Λ^{-1} on the right-hand sides of Eqs. (3.22) and (3.30) arises from the elimination of a fermionic frequency using the rescaled version of the energy-momentum conserving δ -function $\delta_{K'_1 + \dots + K'_n, K_1 + \dots + K_n + \bar{K}_1 + \dots + \bar{K}_m}$. Such a procedure is only meaningful if $z_\psi \leq z_\varphi$, so that bosonic frequencies are not more relevant than fermionic ones. For $z_\varphi \leq z_\psi$ we should use the δ -function to eliminate a bosonic frequency, which amounts to the replacement $\Omega_\Lambda^{-1} \rightarrow \bar{\Omega}_\Lambda^{-1}$ on the right-hand side of Eqs. (3.22) and (3.30). This is the reason for the factor $z_{\min} = \min\{z_\varphi, z_\psi\}$ in Eqs. (3.26) and (3.34).

⁵⁴ L. Hedin, Phys. Rev. **139 A** 796 (1965); L. Hedin and S. Lundquist, *Effects of Electron-Electron and Electron-Phonon Interactions on the One-Electron States of Solids*, in *Solid State Physics*, Vol. 23, edited by F. Seitz, D. Turnbull, and H. Ehrenreich (Academic Press, New York, 1969).

⁵⁵ H. C. Fogedby, J. Phys. C **9**, 3757 (1976).

⁵⁶ D. K. K. Lee and Y. Chen, J. Phys. A **21**, 4155 (1988).

⁵⁷ S. Ledowski, N. Hasselmann, and P. Kopietz, Phys. Rev. A **69**, 061601(R) (2004); N. Hasselmann, S. Ledowski, and P. Kopietz, cond-mat/0409167.

⁵⁸ Note that for $D > 1$ the coupling $\tilde{\gamma}_l$ becomes irrelevant with scaling dimension $-(D-1)/2$. If we formally treat $D-1$ as a small parameter, it might be possible to study the stability of the Luttinger liquid fixed point by means of an expansion in powers of $\epsilon = D-1$. Previously, Ueda and Rice, Phys. Rev. B **29**, 1514 (1984), attempted to construct such an expansion within the field theoretical RG method.

⁵⁹ In deriving Eqs. (4.32) and (4.34), we have set the fixed point value \tilde{r}_* of the relevant coupling \tilde{r}_l equal to zero, which amounts to a re-definition of the bare coupling constant. Otherwise, \tilde{r}_* would explicitly appear in Eqs. (4.32) and (4.34). Setting $\tilde{r}_* = 0$ seems to correspond to the usual normal ordering with respect to the filled Dirac sea in the solution of the TLM via bosonization. In general, the functional dependence of η on the interaction beyond the leading term in the weak coupling expansion depends on the regularization procedure, see H. J. Schulz and B. Sriram Shastry, Phys. Rev. Lett. **80**, 1924 (1998).

⁶⁰ V. Meden pointed out to us that this perfect agreement of Eq. (4.32) with bosonization might no longer occur in the more general TLM with $g_2 \neq g_4$.

⁶¹ T. Busche and P. Kopietz, Int. J. Mod. Phys. B **14**, 1481 (2000).

⁶² B. L. Altshuler, L. B. Ioffe, and A. J. Millis, Phys. Rev. B **50**, 14048 (1994).

⁶³ D. Belitz, T. R. Kirkpatrick, and T. Vojta, Phys. Rev. B **55**, 9452 (1997).

⁶⁴ A. V. Chubukov and D. L. Maslov, Phys. Rev. B **68**, 15113 (2003); A. V. Chubukov, C. Pepin, and J. Rech, Phys. Rev. Lett. **92**, 147003 (2004).

⁶⁵ A. A. Katanin, A. P. Kampf, and V. Yu. Irkhin, cond-mat/0407473.

⁶⁶ L. Bartosch, M. Kollar, and P. Kopietz, Phys. Rev. B **67**, 092403 (2003).

⁶⁷ K. Yang, Phys. Rev. Lett. **93**, 066401 (2004).

⁶⁸ J. Zinn-Justin, *Quantum Field Theory and Critical Phenomena*, (Clarendon Press, Oxford, 4th edition, 2002), chapter 7.3.